Projects Conference

30/6/2021

Abstracts

BME Faculty of Biomedical Engineering
TECHNION - Israel Institute of Technology

Dear all,

We are proud and honored to welcome you to take part in the: ***Annual Project Presentation Conference 2021 of the Biomedical Engineering Faculty***.

This meeting culminates a yearlong research and development experience of our 4th year students. There is a say in Hebrew tradition: "אין חכם כבעל ניסיון", meaning "Experience brings wisdom". This in a nut shell, is what the projects are all about.

During their project development experience, our students had to undergo through all the stages needed to make an idea come true. Starting with a medical problem which they had to tackle, they had to strain their imagination and think "out of the box" in order to come up with a plausible new solution. Then, they had to combine the knowledge they gained during their studies. This knowledge encompasses all the aspects of biomedical engineering, i.e. combining medical background with engineering skills and scientific knowledge. All this package had to be implemented in order to provide a real world solution.

We believe that this hands-on experience exposed and prepared our graduates to the high tech biomedical industry and to a wide variety of biomedical research in a very strong way encouraging multidisciplinary work that is vital for the students' future career, and in addition potentially foster their entrepreneurship skills.

In this booklet the abstracts of all presented projects are displayed for your perusal. We are sure that the students are eager to present the outcome of their year-long projects. We wish all of them rewarding careers after graduation. We hope that very soon they will take an active part in similar projects as professional mentors from both the industry and academia.

Kindest Regards,

Prof. Haim Azhari, Faculty Dean

Prof. Netanel Korin, Course Instructor

List of Abstracts

(1) Continuous, non-invasive and customized hormonal monitoring for women undergoing IVF treatment

Asaf Licht[1], Zinat Awwad[1], Hossam Haick[2]
[1] Faculty of Biomedical Engineering, Technion - IIT, Haifa, Israel
[2] Laboratory for nanomaterial-based devices, Technion - IIT, Haifa, Israel
[3] Harmony

(2) Development of Aligned Automated Scaffolds for Skeletal Muscle Tissue Engineering

Rotem Lootsky[1], Natalie Korlik[1], Margarita Beckerman[1], Hagit Shoyhat[1], Arbel Artzy-Schnirman[1], Shulamit Levenberg[1]
[1] Faculty of Biomedical Engineering, Technion - IIT, Haifa, Israel

(3) Ultrasound Mediated Polymerization for Cell and Drug Delivery

Ruth Potter[1], Yael Dinkevich-Tabory[1], Lior Debbi[1], Majd Machour [1], Oscar Lichtenstein[1], Shulamit Levenberg[1]
[1]Faculty of Biomedical Engineering, Technion - IIT, Haifa, Israel

(4) Higher Functional Connectivity between the Attention and Executive Function Networks after a computerized reading intervention: Evidence For Neural Plasticity Using Functional Magnetic Resonance Imaging (fMRI)

Esti Gitman[1], Carmel Gashri[1], Nikolay Taran[2], Michal Zivan[2] and Tzipi Horowitz-Kraus[2]
[1] Faculty of Biomedical Engineering, Technion - IIT, Haifa, Israel
[2] Educational Neuroimaging Center, Technion - IIT, Haifa, Israel

(5) Image Analysis Of Short-Axis Echocardiography Using Deep-Learning

Lior Drasinover[1], Adi Alfassi[1], Ehud Tal[1], Moti Freiman[1], Dan Adam[1]
[1] Faculty of Biomedical Engineering, Technion - IIT, Haifa, Israel

(6) 3D Force-Based Alternative Keyboard for Myopathic Disease Patients"

Noam Talor[1], Inbal Shafran[1], Gili Kamara[1], Firas Mawase [1]
[1] Faculty of Biomedical Engineering, Technion - IIT, Haifa, Israel

(7) Detection of Arrhythmias Using Wearable Technology

Sagi Ben Itzhak [1], Shir Sharony Ricon [1], Jonathan Sobel [1], Shany Biton [1], Joachim A Behar [1]
[1] Biomedical Engineering Faculty, Technion - IIT, Haifa, Israel

(8) Development of Medical Nanoparticles for the Treatment of Osteosarcoma

Aurelia Sebbane[1], Ariella Chauvart[1], Yakir Amrusi[1], Arbel Artzy-Schnirman[1], Yosi Shamay[1]
[1]Faculty of Biomedical Engineering, Technion – IIT, Haifa, Israel

(9) Cardiovascular Ultrasound Imaging Using Agar Phantom

Anna Yolin[1], Aseel Nama[1], Omri Adler[1], Oscar Lichtenstein [1], Dan Adam [1]
[1] Faculty of Biomedical Engineering, Technion - IIT, Haifa, Israel

(10) Parent-Child Speech Synchrony During a Social Interaction

Fatima Abbas[1], Asrar Khaldey[1], Michal Zivan [2], Tzipi Horowitz-Kraus[1,2]
[1] Faculty of Biomedical Engineering, Technion - IIT, Haifa, Israel
[2] Faculty of Education in Science and Technology, Technion - IIT, Haifa, Israel

(11) Brain Tumor Segmentation using Deep Learning Methods

Hadas Ben Atya[1], Ori Rajchert[1], Moti Freiman[2]
[1]Faculty of Biomedical Engineering, Technion - IIT, Haifa, Israel
[2]Technion Computational MRI Lab (TCML), Technion - IIT, Haifa, Israel

(12) Reorganization of Functional Networks Following MRI-Guided Focused Ultrasound Treatment in Essential Tremor Patients

Iyar Hadad[1], Naama Rivlin[1], Gil Zur[2], Noam Bosak[3], Firas Mawase[1]
[1]Faculty of Biomedical Engineering, Technion - IIT, Haifa, Israel
[2]Department of Radiology, Rambam Health Care Campus
[3]Department of Neurology, Rambam Health Care Campus

(13) AI Based Decision Support System for Labor and Delivery Management

Amit Parizat[1], Rotem Shapira[1], Noam Keidar[1,2], Joachim Behar[1], Yael Yaniv[1]
[1]Faculty of Biomedical Engineering, Technion - IIT, Haifa, Israel
[2]Faculty of Medicine, Technion - IIT, Haifa, Israel

(14) Optimizing Immune Cell Tracking Methods for Multimodality Imaging

Sivan Barash[1], Shachar Zigron[1], Moti Freiman[1], Katrien Vandoorne[1]
[1] Faculty of Biomedical Engineering, Technion - IIT, Haifa, Israel

(15) Identification of Candidate Chronotherapeutic Drugs Through Their Molecular Targets

Ofek Aloush[1], Shahaf Karpenkop[1,2], Jonathan Sobel[1], Joachim Behar[1]
[1]Faculty of Biomedical Engineering, Technion - IIT, Haifa, Israel
[2]Faculty of Medicine, Technion - IIT, Haifa, Israel

(16) Characterization of Cell Assembly and Electrophysiological Properties in Engineered Heart Slices

Lior Haim[1,2], Nir Litver[1,2], Arbel Artzi Schnirman[1], Matteo Ghiringhelli[2], and Lior Gepstein[2]
[1] Faculty of Biomedical Engineering, Technion - IIT, Haifa, Israel
[2] Ruth and Bruce Rappaport Faculty of Medicine, Technion - IIT, Haifa, Israel

(17) Plasticity of Synapses in Zebrafish Larvae due to Epileptic Seizures

Avigail Berger[1,2], Noya Zeret[1,2], Ory Perelsman[1], and Limor Friefeld[1]
[1] Faculty of Biomedical Engineering, Technion, Haifa, Israel
[2] Faculty of Medicine, Technion, Haifa, Israel

(18) Predictive Model for Core Temperature from Thermal Face Images

Avraham Tenenbaum[1,2], Sivan Geva[1,2], Nati Daniel[2], Yonatan Savir[2]
[1] Biomedical Engineering Faculty, Technion - IIT, Haifa, Israel
[2] Faculty of Medicine, Technion - IIT, Haifa, Israel

(19) HRV-CAM: A Novel Approach for Remote Detection of Cardiac Arrhythmias

Yonathan Belicha[1], Daniel Cherniavsky[1], Moran Davoodi[1], Joachim Behar[1], Yael Yaniv[1]
[1]Faculty of Biomedical Engineering, Technion - IIT, Haifa, Israel

(20) Compact Spectrally Encoded Interferometry Probe for Imaging the Acoustic Reflex In Humans

Chen Berkovich[1], Rahel Rosen[1], Lidan Fridman[1], Matan Hamra[1], Dvir Yelin[1]
[1]Faculty of Biomedical Engineering, Technion – IIT, Haifa, Israel

(21) The effects on uncertainty and frequency of movements on their representation in the motor cortex: a TMS study

Matitiahu Gorodetsky[1], Marvyn Bebar[1], Abed Suleiman[1], Firas Mawase[1]
[1]Biomedical Engineering Faculty, Technion - IIT, Haifa, Israel

(22) Bioreactor Design for Selective Differentiation of Stem Cells to Engineer a Thick, 3D Muscle and Adipose Tissue

Oryan Karni[1], Francesca Jaffe [1], Yedidya Zagury [1], Arbel Artzy-Schnirman[1], Shulamit Levenberg[1]
[1] Biomedical Engineering Faculty, Technion - IIT, Haifa, Israel

(23) Design, Development and Testing of a New Polymeric Heart Valve

Gal Pereg[1], Yevgeniy Kreinin[1], Oscar Lichtenstein[1], Netanel Korin[1]
[1]Faculty of Biomedical Engineering, Technion - IIT, Haifa, Israel

(24) Development of a Spheroid Model that Simulates Drug Penetration in Solid Tumors

Or Levy[1], Orel Shahadi[1], Maytal Avrashami[1], Hagit Sason-Bauer[1], Arbel Artzy-Schnirman[1], Yosi Shamay[1]
[1]Faculty of Biomedical Engineering, Technion - IIT, Haifa, Israel

(25) Brain tumors segmentation from MRI data with deep-learning

Elinoy Faibish[1], Matan Kachel [1], Moti Freiman[1]
[1] Faculty of Biomedical Engineering, Technion - IIT, Haifa, Israel

(26) Infant Hearing Test Using Eye Tracking

Suzan Shehady [1], Nardeen Badarny[1], Dr. Rola Farah[2] and Dr. Michal Zivan[2]
[1] Faculty of Biomedical Engineering, Technion
[2] Faculty of Education in Science and Technology, Technion

(27) Automatic Detection of LUS Characteristics and Specifically COVID-19 Related LUS Artifacts

Dekel Brav[1], Ehud Tal[1], Noy Mark[1], Lior Lupu[2], Dan Adam[1]
[1]Faculty of Biomedical Engineering, Technion - IIT, Haifa, Israel
[2]Department of Cardiology, Tel Aviv Sourasky Medical Center

(28) Red Blood Cell Based Drug Carriers for Targeted Delivery to Stenotic Arteries - an in Vitro Study

Shay Ohana[1], Ofir Kalman[1], Danielle Nemcovsky-Amar[1], Maria Khoury[1], Oscar Lichtenstein[1], Netanel Korin[1]
[1]Faculty of Biomedical Engineering, Technion - IIT, Haifa, Israel

(29) Suppressing the Reflex Response by Exposure to Weak Pre-Pulse in the Startle Circuit of the Larval Zebrafish

Asaf Tzur[1], Yakir Yemini[1], Dor Meron[1], Michal Zivan[1], Limor Freifeld[1]
[1]Faculty of Biomedical Engineering, Technion - IIT, Haifa, Israel

(30) The Opposing Effects of Hematopoietic Glucose Uptake for Leukocyte Production in Diabetes and G-CSF Treatment by Retrospective 18F-FDG PET/CT Analysis

Bashar Shehadeh[1], Adi Daoud[1], Katrien Vandoorne[1], Michal Weiler-Sagie[2]
[1]Faculty of Biomedical Engineering, Technion - IIT
[2]Nuclear Medicine Department, Rambam Health Care Campus, Haifa, Israel

(31) System development for ECG noise sources detection and classification in Electrophysiology labs during clinical operations of heart arrhythmia patients

Nitzan Gorani[1], Gaia Levin[1], Tsafrir Ozer[2], Firas Mawase[1]
[1]Faculty of Biomedical Engineering, Technion - IIT, Haifa, Israel
[2]Biosense Webster company part of J&J family, Yokneam, Israel

(32) A Whole-Cell Bacterial Biosensor for L-lactate Detection in Urine

Rami Eid[1], Jawan Asla[1], Valeriia Kravchik[1], Ramez Daniel[1]
[1] Faculty of Biomedical Engineering, Technion - IIT, Haifa, Israel

(33) Evaluation Of Mental States with a Mood Tracking Smartphone App

Daniel Sapir[1], Menucha Meir[1], Miri Cohen[2], Yossi Shamay[1]
[1] Biomedical Engineering Faculty, Technion - IIT, Haifa, Israel
[2] Faculty of Social Welfare and Health, University of Haifa, Israel

(34) Preparation of Nanoparticles for KRAS P53 Derived Lung Cancer

Liana Shalabi[1], Salma Khateeb[1], Yuval Harris [1], Arbel Artzy-schnirman[1], Yosi Shammy[1]
[1]Biomedical Engineering Faculty, Technion - IIT, Haifa, Israel

(35) Detecting Stenosis in the Carotid Arteries Based on SCG and Acoustic Signals

Elias Bisharat[1], Noa Bachner-Hinenzon[2], Oscar Lichtenstein[1]
[1]Faculty of Biomedical Engineering, Technion - IIT, Haifa, Israel
[2]Sanolla, Nesher

(36) Semi-automatic Classification of the COVID-19 disease based on Lung Ultrasound

Mor Ventura[1], Omri Magen[1], Ehud Tal[1], Noy Mark[1], Lior Lupu[2], Dan Adam[1]
[1]Faculty of Biomedical Engineering, Technion - IIT, Haifa, Israel
[2]Department of Cardiology, Tel-Aviv Sourasky Medical Center

37) Modeling of biological processes using subthreshold electrical circuits

Marah Matar[1], Bayan Khalil[1], Ilan Oren[1], Daniel Ramez[1]
[1]Faculty of Biomedical Engineering, Technion - IIT, Haifa, Israel

38) Determining the Involvement of the Future-Reading Network in Processing Narratives from Age 5 to 18 Years Using Functional Connectivity Approach

Narmeen Haj[2], Tamara Rohana[2], Raya Meri[1], Michal Zivan[1], Tzipi Horowitz-Kraus[1,2]
[1]Educational Neuroimaging Center, Faculty of Education in Science and Technology, Technion – IIT, Haifa, Israel
[2]Faculty of Biomedical Engineering, Technion – IIT, Haifa, Israel

(1)

Continuous, non-invasive and customized hormonal monitoring for women undergoing IVF treatment

Asaf Licht[1], Zinat Awwad[1], Hossam Haick[2]

[1] Faculty of Biomedical Engineering, Technion - IIT, Haifa, Israel
[2] Laboratory for nanomaterial-based devices, Technion - IIT, Haifa, Israel
[3] Harmony

Introduction:

For effective in-vitro fertilization (IVF) treatments, physicians need comprehensive monitoring of two hormonal levels: Estradiol and Progesterone. Today, this is done by conducting several blood tests a week. However, when trying to monitor continuous hormonal changes with un-continuous methods, like blood tests, some clinical data is missed affecting the efficiency of the giving treatment. Also, blood tests are an unpleasant, invasive, and time-consuming process. COVID-19 pandemic has empowered the need for remote patient monitoring (RPM) – 30M US patients will use RPM tools by 2024.

We aim to develop a product that will allow continuous remote hormonal monitoring based on sampling VOCs profile from females' skins. To do so we have two main hypotheses:

1. There is a correlation between the VOCs profile and the hormonal profile.
2. Today's technology can detect the VOCs profile and is sensitive to its changes.

Method:

To prove the first hypothesis, we relied first on earlier works described in the literature that claims that a woman's odor varies depending on the hormonal changes. Later, we designed a clinical experiment that aims to empower the correlation: VOCs profile will be collected from the human-female body using Tenax (porous polymer adsorbent patches). We will analyze the samples with the GC-MS method and a laboratory electronic-nose-system, and compare it to the hormonal levels.

To prove the second hypothesis, we selected 3 types of VOCs from different chemistry groups we identified via literature. Those chemicals were bought and vaporized using a "bubbler" machinery, then carried with a carrier gas (nitrogen) into a close chamber containing 13 chemo-sensors with several types of chemistries. The measures occurred in different concentrations of the VOC.

Results:

- We found via literature several VOCs that have a correlation with sex-hormones, including the hormones' metabolic derivatives and molecules formed as part of hormone-related physiological responses.
- We established a collaboration with the IVF department in Sheba Medical Center to conduct a clinical 100-participant-experiment- includes fund. Budget and Helsinki approvals have been received.

- We sampled VOCs from a woman's body and performed preliminary tests using GCMS methods. Then adjusted the test methodology to suit the designed experiment data. Also, we succeeded to verify the presence of some of the molecules, described in the literature, on the woman's skin.
- By exposing the sensors to one of the molecules (graph 1), we found that out of the 13 tested sensors, 7 of them showed a qualitative and quantitative response.

Conclusions:

- There is a correlation between VOCs profile from the skin and the hormonal levels in the blood. To widen and empower the correlation, the designed experiment is needed.
- The sensors can detect the VOCs and are also sensitive to the changes in their **physiological** concentrations.
- Due to the different reactivity of the sensors, it seems that there is a differentiation ability between the different molecules. To confirm this, a further experiment is planned.
- The need for such technological advancement is critical in terms of clinical data, patient convenience, and market needs.

Keywords: Hormones, VOCs, Chemo-sensor, IVF.

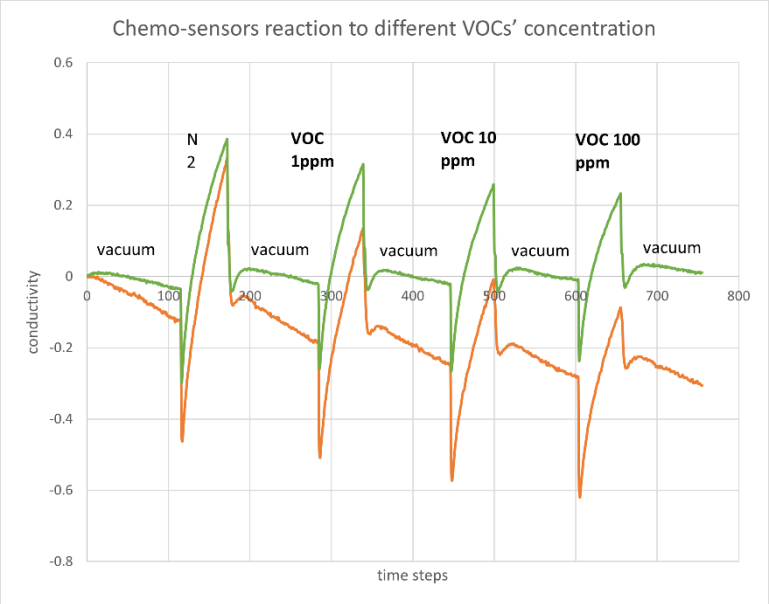

Fig1. Description: The conductivity of 2 different chemo-sensors is presented. The exposures to the different VOC concentrations are marked by their concentration on the graph. As we can observe one of the sensors has a change in its conductivity only when exposed and measured, while the second's conductivity is decreasing continuously but with very clear peaks observations when exposed to the VOC. Each of the sensors allows the measurement of the VOC concentration changes – while the combination of both sensors enabling to differentiate in a better resolution and certainty.

(2)

Development of Aligned Automated Scaffolds for Skeletal Muscle Tissue Engineering

Rotem Lootsky[1], Natalie Korlik[1], Margarita Beckerman[1], Hagit Shoyhat[1], Arbel Artzy- Schnirman[1], Shulamit Levenberg[1]

[1] Faculty of Biomedical Engineering, Technion - IIT, Haifa, Israel

Introduction

Skeletal muscle (SkM) tissue engineering (TE) offers a solution to muscle regeneration following tissue loss. The current treatment is an autologous flap taken from a different site in the body, which yields limited degree of success. TE consists of *in-vitro* fabrication of a 3D tissue construct which will be implanted in the damaged muscle. A primary component of this construct is the scaffold, a 3D platform, providing cells structural support and directs tissue development. Scaffolds with geometry that matches the structure of the native SkM, will guide the formation of the tissue. To address this need we designed and developed an automated method to create an aligned and porous scaffold using indirect 3D printing. The common methods used today, are not automated and include many steps which results in scaffolds that vary greatly leading to reduced reproducibility.

Methods

Scaffolds with directed channels were designed in SolidWorks and created using an indirect 3D printing technique. A mold made of sacrificial material, BVOH, was created using a standard extrusion 3D printer. Various prototypes were designed, and different parameters were tested, to allow maximal cell attachment and spread. The different molds were filled with a polymeric solution, in different concentrations and organic solvents. Then the molds were frozen in different temperatures and lyophilized to remove the solvent. Next, the molds were dissolved in water to obtain the scaffolds that were imaged with SEM to determine porosity distribution. The scaffolds were seeded with skeletal muscle cells and cultured for 10-21 days. Cell differentiation and tissue formation were evaluated with immunofluorescent staining and confocal microscopy.

Results

To fabricate suitable scaffold for cell attachment and spread, several designs and factors were evaluated. The best mold was a continues tube, rather than individual inserts. The desired pore distribution was achieved using a 5% solution of PLLA/PLGA W/V prepared in dioxane and higher freezing temperature. Cells were seeded on the fabricated scaffolds, and immunofluorescent stain of myotubes reveled the cells followed the direction of the channels and differentiated along them.

Conclusions

We successfully developed an automated aligned porous scaffold compatible for SkM-TE. We fabricated a printed mold with specific channels morphology, using BVOH, a water-soluble material and standard extrusion 3D printer. This method is repetitive and results in automated aligned scaffolds which can then be used as ideal constructs for muscle tissue engineering. In addition, different parameters can be changed such as freezing temperature to achieve better porosity according to the cells used. Moreover, BVOH is inert to organic solvents, therefore can be used with a variety of polymer solutions and printed in different geometries according to the desired use.

Keywords

Muscle tissue engineering, Muscle loss, Indirect 3D printing, Aligned scaffold

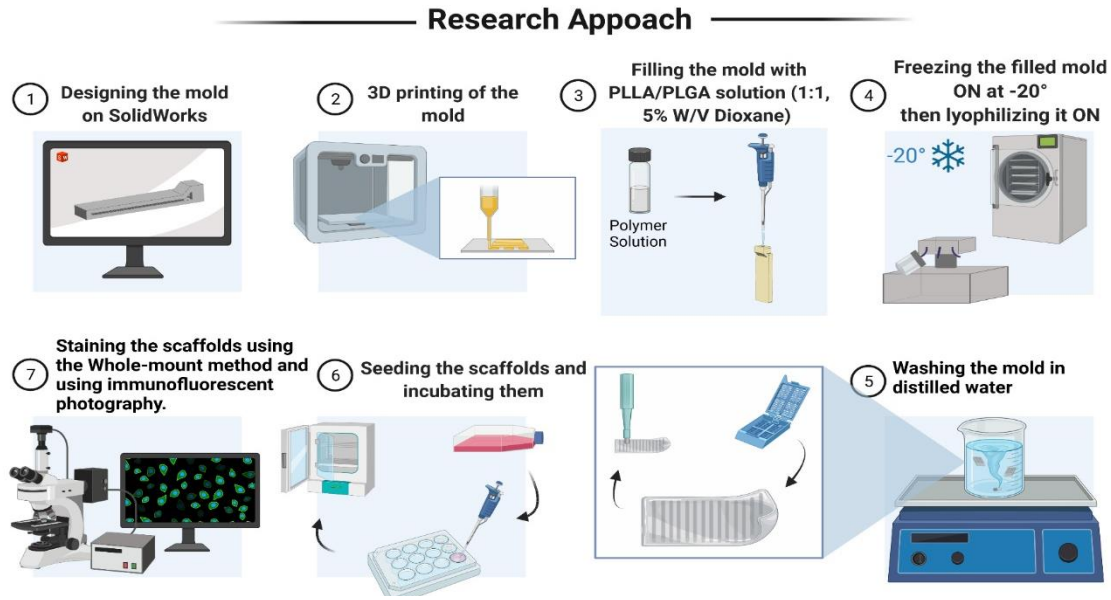

Figure 1- Flow chart describing the method used in the project.

(3)

Ultrasound Mediated Polymerization for Cell and Drug Delivery

Ruth Potter[1], Yael Dinkevich-Tabory[1], Lior Debbi[1], Majd Machour [1], Oscar Lichtenstein[1], Shulamit Levenberg[1]

[1]Faculty of Biomedical Engineering, Technion - IIT, Haifa, Israel

Introduction: Organ transplantation is a standard practice in modern medicine to treat patients experiencing organ failure. The major drawback of this method is the lack of human donors, creating a market demand for an alternative source of organ substitutes. Recent advances in the tissue engineering field have shown that 3D bio-printing may hold the key to producing lab-grown functional organs, reducing the demand for human donation. This bio-printing approach requires an invasive surgical procedure for implantation of the construct. To overcome this problem, recent studies presented *in-vivo* hydrogel polymerization of cell-infused scaffolds as a method for non-invasive 3D bioprinting of tissue constructs using near-infrared light (NIR). This method can be used for superficially injected constructs only, reaching a few centimeters under the skin. A need arises for an approach to polymerize scaffold materials in areas deep inside the body. This leads to the development of acousto-sensitive materials controlled by existing ultrasound technology, known to be safe and effective for non-invasive procedures. Such acousto-sensitive materials show promise for controlled and targeted drug release applications as well as cell delivery and non-invasive 3D bioprinting.

Methods: Cross-linking of polyethylene glycol diacrylate (PEG-DA) was performed by ultrasound waves. A 10% PEG-DA solution was prepared in small glass vials. Argon gas was applied for 45 seconds to the solution driving off the oxygen. Next, the solution was exposed to ultrasound waves causing polymerization to form a bio-hydrogel. To create hydrogels with variable stiffnesses, different intensities of ultrasound were applied for different exposure times. This range of stiffnesses was measured using a rheometer. A variation of the protocol used PVA-MA solution instead of PEG-DA, providing a range of materials with different properties.

This hydrogel polymerization protocol using ultrasound was developed for two applications: cell delivery and drug delivery. For the cell delivery application, the protocol was performed to prove biocompatibility by adding dental pulp stem cells (DPSCs) to the PEG-DA solution. To enhance viability, the DPSCs were encapsulated in beads of alginate using a micro-fluid encapsulation technique before addition to the PEG-DA. After ultrasound exposure, a live-dead assay was performed to show cell viability. For the drug delivery application, a drug release profile was

built, recording the release of bovine serum albumin (BSA) from polymerized PEG-DA hydrogels with different stiffnesses using a Bradford assay.

Results: Mechanical profiles showed a correlation between the ultrasound intensity level or ultrasound exposure time and the hydrogel stiffness. The values calculated include stress-strain curve, Young's modulus, yield point and energy loss. The live-dead assay showed high viability of cells throughout the polymerization process, reaching an average of 88.88% viability when using ultrasound intensity of $0.5\ W/cm^2$ for 20 seconds. The Bradford assay showed a correlation between hydrogel stiffness and drug release rates.

Conclusions: Polymerization of bio-compatible hydrogels can be induced using ultrasound. This method can be used to deliver the materials for a hydrogel scaffold deep within the body using a minimally invasive procedure. The scaffold can be infused with cells, forming a 3D structure on which they can grow into a tissue or organ. Alternatively, the scaffold can contain drugs delivered to a specific site at a controlled release rate.

Keywords: Ultrasound, in-situ bioprinting, tissue engineering, controlled drug release

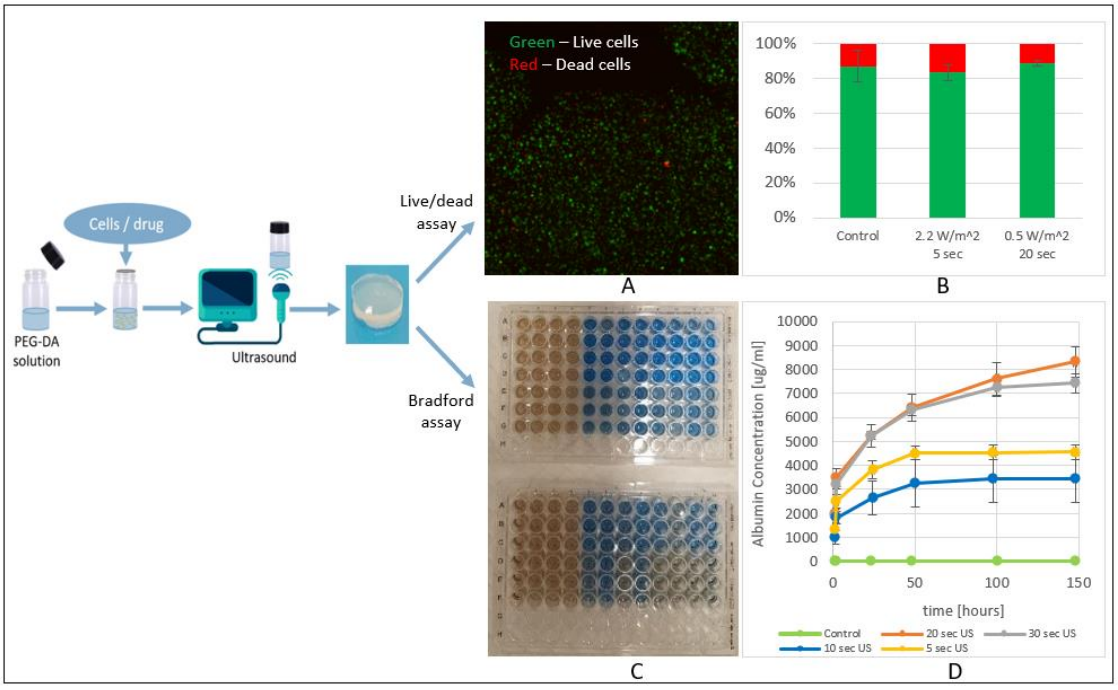

Figure 1 - Schematic illustration of the experiment. A) Live/dead assay after exposure to ultrasound at 0.5 W/m^2 for 20 seconds. B) Average results from live/dead assays for different ultrasound intensities. Green – live cells, Red – dead cells.
C) Bradford assay for albumin release for different lengths of ultrasound exposure at intensity 2.2 W/m^2. D) Average albumin release over one week during Bradford assay

(4)

Higher Functional Connectivity between the Attention and Executive Function Networks after a computerized reading intervention: Evidence for Neural Plasticity Using Functional Magnetic Resonance Imaging (fMRI)

Esti Gitman[1], Carmel Gashri[1], Nikolay Taran[2], Michal Zivan[2] and Tzipi Horowitz-Kraus[2]

[1] Faculty of Biomedical Engineering, Technion - IIT, Haifa, Israel
[2] Educational Neuroimaging Center, Technion - IIT, Haifa, Israel

Introduction: Developmental dyslexia is a reading impairment which is manifested during early school age years. The reading difficulties of children with dyslexia include low reading speed and inaccuracy. Children with dyslexia experience unwanted visual symptoms while reading. The abovementioned symptoms and difficulties have an emotional impact on children with dyslexia, as they usually suffer from negative prejudice from their peers.

Current interventions for dyslexia, based on phonological aspects, have not been approved to be fully effective. In this project, we would like to test the effectiveness of an executive-function based intervention. This intervention targets the visual-attention component by driving the child to read a text at a fast pace, as the letters are being deleted. We would like to understand the effect of this intervention on the set of brain networks related to reading, with an especial focus on visual attention- the dorsal attention network and the ventral attention network.

Methods: 80 children in the ages of 8-12 (44 typically reading and 36 with dyslexia) participated in the experiment. First, the children underwent a set of cognitive and behavioral tests. After they were evaluated, they performed a reading fluency task under fMRI scan in two conditions- a Still condition, in which a story appeared stationary on the screen and a Deleted condition, in which the story was deleted letter-by-letter. The participants were divided into two groups, each group underwent a different intervention method. One group underwent an executive-function based reading intervention and the other group underwent a math intervention as a control condition. Afterwards, they were re-examined using the same behavioral tests and fMRI session.

Results: Before the intervention, children with dyslexia performed poorly in reading comprehension, visual-attention and executive function tasks in comparison to typically reading children. In the pre-post intervention comparison, we found that children with dyslexia that underwent the executive function-based reading intervention, had an improvement in reading comprehension and executive function tests, when compared to those who did math training. In addition, we found higher functional connectivity between the ventral attention network and the fronto-parietal network in children with dyslexia after the reading intervention. When analyzing the post-intervention fMRI data alone, we found that children with dyslexia showed lower functional connectivity within the dorsal attention, while reading Still text, compared to typically reading children.

Conclusions: The presented findings suggest that the executive-function based intervention effectively improves the reading skills of children with dyslexia by causing an improved integration of executive functions and visual-attention processes for children with dyslexia.

Keywords: Dyslexia, Dorsal Attention Network, fMRI, Functional Connectivity

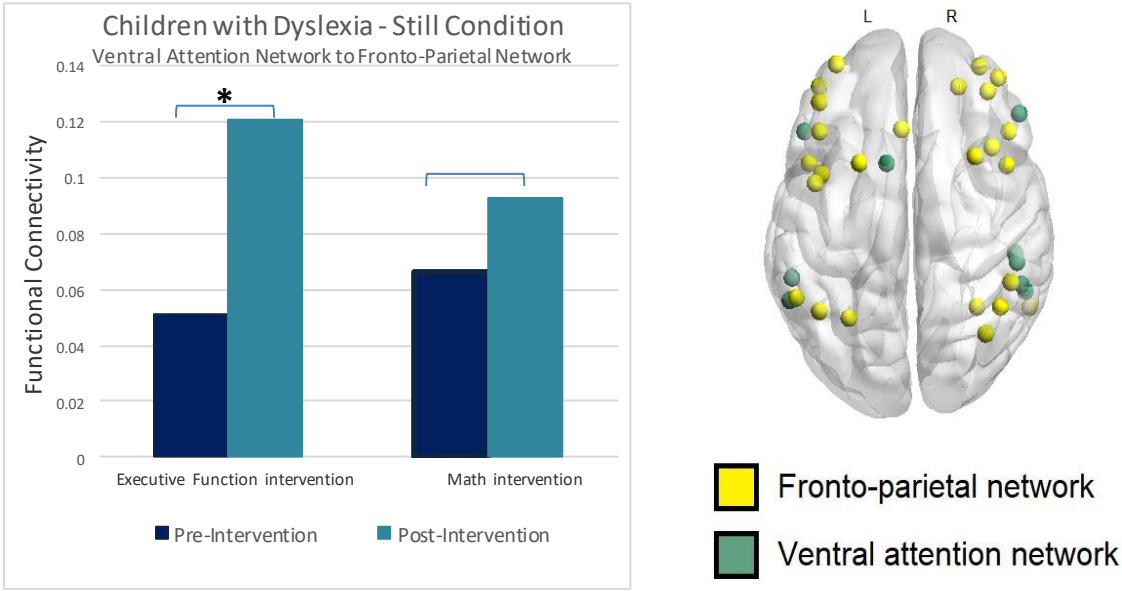

Figure 1: Left - Pre-Post intervention comparison in children with dyslexia. Only in the Executive Function-based reading intervention there were significant differences (* - $p<0.05$, n.s – non significant). Right – the Ventral Attention and Fronto-Parietal networks.

(5)

"Image Analysis Of Short-Axis Echocardiography Using Deep-Learning"

Lior Drasinover[1], Adi Alfassi[1], Ehud Tal[1], Moti Freiman[1], Dan Adam[1]

[1] Faculty of Biomedical Engineering, Technion - IIT, Haifa, Israel

Introduction: Echocardiography is a widely used imaging, that allows for a qualitative and quantitative evaluation of the heart's physiology and function. This common exam is analyzed by physicians, which can cause them significant strain and may lead to misdiagnosis. In addition, most studies conducted regarding analysis of clinical parameters from Echocardiography are focused on Long-Axis views of echocardiography, while important clinical parameters can be detected from Short-Axis views as well. Here we developed a fully- automatic tool for classification and segmentation of the LV in short axis echocardiographic views; namely, the LV wall (i.e., myocardium). This tool can raise the overall quality of the diagnostic process by including unexplored clinical information, as well as providing faster and uniform analysis.

Methods: 500 Short-Axis Echocardiography recordings (including recordings of all 3 views- Apex, Papillary and Base) were classified according to the correct view and segmented using semi-automatic software tool (EchoPac by GE medical). This data used as a segmented dataset used for supervised learning. A classification model was then built and used as a feature extractor and trained to classify among the 3 views, using 5 frames of equal time differences. Afterwards, a segmentation model was built as a U-NET. This model uses 3 frames around the end-systolic frame (detected automatically by the EchoPac tool) and results a binary mask of "LV" and "no- LV" (derived from a probability map). The segmentation model was trained in 3 learning strategies: Training the model on our dataset without use of previous weights, Training the model on our dataset using weights taken from a similar model trained on a different dataset, and training the model on our dataset using weights from the classification model trained on our dataset.

Results: The Classification Model resulted a 60% accuracy. The different segmentation learning strategies resulted Dice Score of over 0.7 and showed an improving learning process. The learning strategy of using weights from the classification model resulted the best Dice Score (0.727) and the best visual fit to the ground truth. The strategy of using weights from a model trained on different dataset resulted the smallest loss but had the worse Dice Score and visual fit.

Conclusions: The U-NET and the different segmentation learning strategies succeeded in learning the dataset despite the small, difficult dataset, and their learning processed can improve. The best learning strategy for our dataset is transfer learning: using weights from a model that was trained on the same domain (classification model trained on our dataset).

Keywords: Echocardiography, Deep learning, Segmentation, Classification

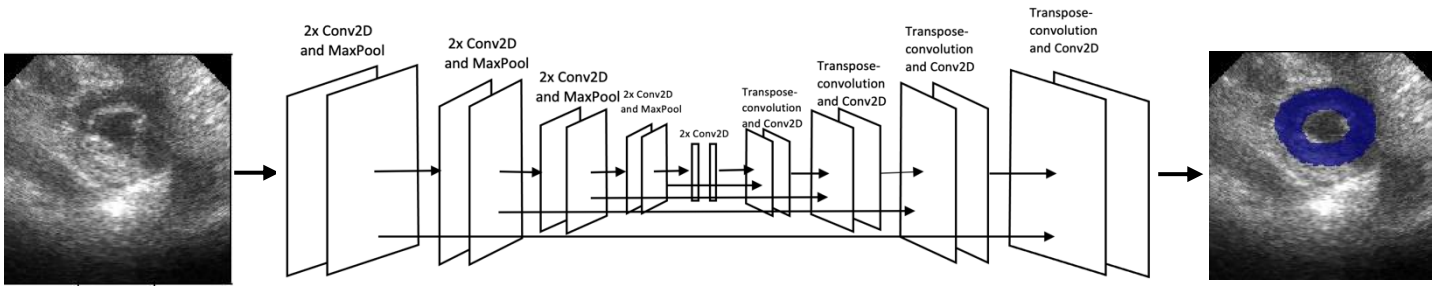

Figure 1: The UNet segmentation model-The model's input is a short-axis recording, and the output would be the same recording with a visible mask represents the segmentation of the LV muscle. The model includes 5 Convolutional levels and 4 Transpose Convolutional levels, while each Transpose Convolutional level receives as an input data from both previous level and the matching Convolutional level.

(6)

3D Force-Based Alternative Keyboard for Myopathic Disease Patients

Noam Talor[1], Inbal Shafran[1], Gili Kamara[1], Firas Mawase[1]

Faculty of Biomedical Engineering, Technion - IIT, Haifa, Israel

Introduction:

Computer usage is an integral part of daily life in the digital age. The main input interfaces of the computer are mouse and keyboard, which require gentle and precise finger movements. People who suffer from neurological or muscular diseases, such as muscular dystrophy, have difficulties in performing the necessary movements for standard keyboard usage. Muscular dystrophy diseases are manifested by increasing weakness accompanied by loss in muscle mass. These diseases are characterized by muscle tissue degeneration and caused by genetic mutations that interfere with protein production, which are essential for the construction and healthy function of the muscle tissue. The main difficulty of these people regarding keyboard usage, is the need to perform small, delicate movements over the keyboard.

We designed and built a force sensor-based keyboard that does not require finger movements, but instead works by applying force in different directions. The keyboard is suitable for people with muscular degeneration diseases, by eliminating the need to raise the fingers and move them over the keyboard.

Methods:

We designed a keyboard based on 3D FSR, one sensor per finger (i.e., 10 sensors). The sensors are integrated into an agronomically designed appliance, which allows the user to place his finger directly above the designated sensor. Typing is executed by rolling the fingers on top of the sensor. Each roll to any distinct direction (up, down, left, and right) will type a single key (i.e., 4 keys). The sensors are connected to an Arduino DUE hardware. The input from the Arduino is processed and performs the desired typing command.

Results:

A one finger model was printed using a "Formlabs" 3D printer, and a sensor was integrated in it. The forces measured by the sensor are processed using the Arduino and a software written in C, to discern between different movement types, thereby enabling the typing of 4 keys from a single sensor.

Conclusions:

The accuracy achieved, along with the fact that the appliance is built of affordable and approachable hardware, software, and materials, enable an applicable solution that meets the basic need of typing for people who suffer from motor disabilities in their hands.

This provides a proof of concept for a full keyboard using all 10 fingers. An extension of the appliance needs to be done for 10 fingers.

Keywords: Myopathic Disease, 3D FSR, Arduino, Keyboard

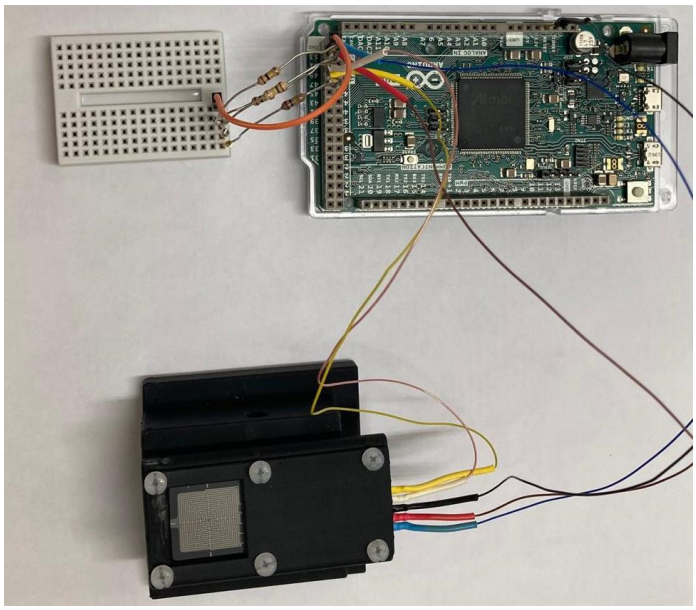

Figure 1: Keyboard prototype for one finger

(7)

Detection of Arrhythmias Using Wearable Technology

Sagi Ben Itzhak[1], Shir Sharony Ricon[1], Jonathan Sobel[1], Shany Biton[1], Joachim Behar[1]

[1]Biomedical Engineering Faculty, Technion - IIT, Haifa, Israel

Introduction: Arrhythmias are abnormal cardiac rhythms that affects the pattern and rate of the heartbeat. To date, electrocardiogram (ECG) feature analysis is considered the gold standard for the diagnosis of arrhythmias. With the rising popularity of wearable devices, arrythmia detection based on wearable technology have the potential to significantly increase the early detection of arrhythmias and facilitate their monitoring.

Our goal is to develop an algorithm for detection and classification of arrhythmias that relies solely on data extracted from wearable devices.

Methods:

The University of Virginia Database (UVAF) contains n=2891 annotated recordings from individual patients. Each recording consists of raw continuous ECG of approximately 24 hours, beat-to-beat (RR) interval time series, and rhythm type for each heartbeat. The typical time resolution of heart rate measurements available from wearable devices varies from five seconds to several minutes depending on the device. To simulate the data provided by wearable devices, the average heart rate (HR) was computed for non-overlapping windows for different resolutions (i.e. windows of length 5, 15, 30,60, 300, or 600 seconds). The classification task included four rhythm types: normal sinus rhythm, atrial fibrillation, sinus bradycardia, and supraventricular tachyarrhythmia. A total of 15 features were engineered based on the window averaged HR time series. The classification was performed at two levels: patient level and segment level. At the patient level, each patient was classified with an overall rhythm label based on the entire 24 hours of data. For the segment level patient's data was divided into segments of 60 minutes. Each segment was then classified separately, independent from the other segments. For each classification level and resolution three multiclass classification models were trained: Logistic Regression (LR), Support Vector Machine (SVM) with RBF kernel, and Random Forest (RF). A total of 30 experiments were performed (Figure 1).

Results:

The RF classifier achieved the best performance with an average accuracy of 94.8%, average F1 score of 93.4%, and average AUROC of 96.2% at the segment level. The performance of the Logistic regression classifier was significantly lower compared to

the non-linear models (RF, SVM), achieving an average F1 score of 87.4% at the segment level.

The performance of all three models decreased with the increase of the window size. A significant decrease of performance was noticeable only on classification of AF patients.

Conclusions:

The results obtained by the non-linear models indicate that it is not only possible to distinguish the healthy patients from the arrhythmia patients, but they can also accurately distinguish between the three types of arrhythmias included in the experiments. AF is characterized by chaotic rhythm and large variance between proximate heartbeats. The detection of those characteristics is dependent on the data resolution, resulting in the decrease in the performance of the models with the decrease of the window resolution.

Keywords: Arrhythmias; Atrial Fibrillation; Machine Learning; We

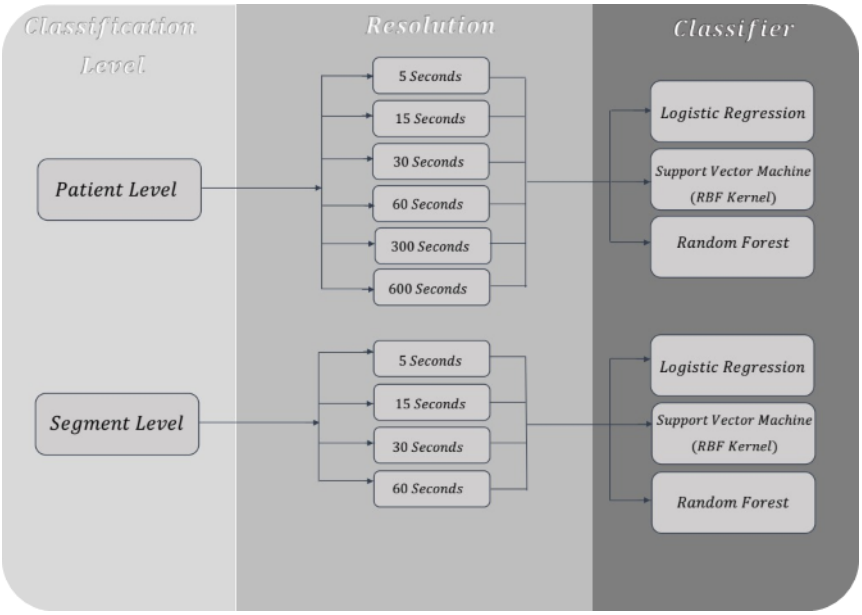

(8)

Development of Medical Nanoparticles for the Treatment of Osteosarcoma

Aurelia Sebbane[1], Ariella Chauvart[1], Yakir Amrusi[1], Arbel Artzy-Schnirman[1], Yosi Shamay[1]

[1]Faculty of Biomedical Engineering, Technion – IIT, Haifa, Israel

Introduction: Osteosarcoma is an aggressive bone-forming tumor that can develop in different parts of the skeleton. It is often accompanied by the spread of micro-metastases and shows a low survival rate.

To this day, the accepted treatment for osteosarcoma is a combination of surgery and chemotherapy which causes severe side effects.

Therefore, there is a significant need to find a more effective and complete treatment. Since the genetic origin of osteosarcoma remains unknown and undefined, today, the interest is focused on drugs that have been proven effective against other types of cancer. The goal is to find a combination of therapies that will impair the mechanisms that give osteosarcoma cells their resistance to existing chemotherapy and therapies.

We based our research on the ability of certain drugs to form stable nanoparticles with the correct stabilizer. Indeed, the said nanoparticles would contain an optimal combination and concentration of anti-cancer drugs and would allow to improve and control the delivery of the drugs to the tumor site, as well as reduce side effects.

In parallel, we tested those nanoparticles on cancerous cells in two-and-three-dimensional experiments. The objective was to mimic a tumor in the most accurate way possible in order to get a sense on the efficiency of the experimental treatment.

In this project, we focused our research on the MG-63 osteosarcoma cell line.

Methods: We first prepared nanoparticles by mixing the drug of interest or combination of drugs with a solution of sodium bicarbonate and stabilizer of our choice. We tested about a dozen of different anti-cancer drugs both alone and in combinations of which we tried to optimize the ratio.

The nanoparticles were then purified using either centrifugation or PD10 size exclusion chromatography.
Next, we examined and evaluated the quality of our nanoparticles using DLS. Particle size, distribution and stability over time were measured. Lastly, in order to evaluate the efficacity of the different nanoparticles and compare it to the free drug's, we performed 2D and 3D cell viability assays on MG-63 cancer cells using ULA plates. We observed the uptake and anti-cancer activity of the NPs on the cells' viability using LionHeart automated fluorescence microscope.

Results: 2D cell viability assays showed that a majority of our nanoparticles inhibited the growth of the cancer cells. Among them, two combinations proved to be more efficient and even considerably decreased the viability of the cells: Palbociclib (70%) with Sorafenib (30%) and Palbociclib (40%) with Carfilzomib (60%). However, the 3D assay did not fully confirm the said efficiency: the nanoparticles only partially attack the cells on the outer shell of the spheroids and did not penetrate them.

Conclusions: The heterogenicity of osteosarcoma makes it almost imperative to personalize the treatment for each cell line. Palbociclib, sorafenib and carfilzomib different combinations proved to produce stable nanoparticles and presented encouraging anti-cancer effects in 2D experiments. Future work would investigate the capacity of the nanoparticles to invade spheroids to the core.

Keywords: Nanoparticles, Personalized cancer drug delivery, MG-63 cell line

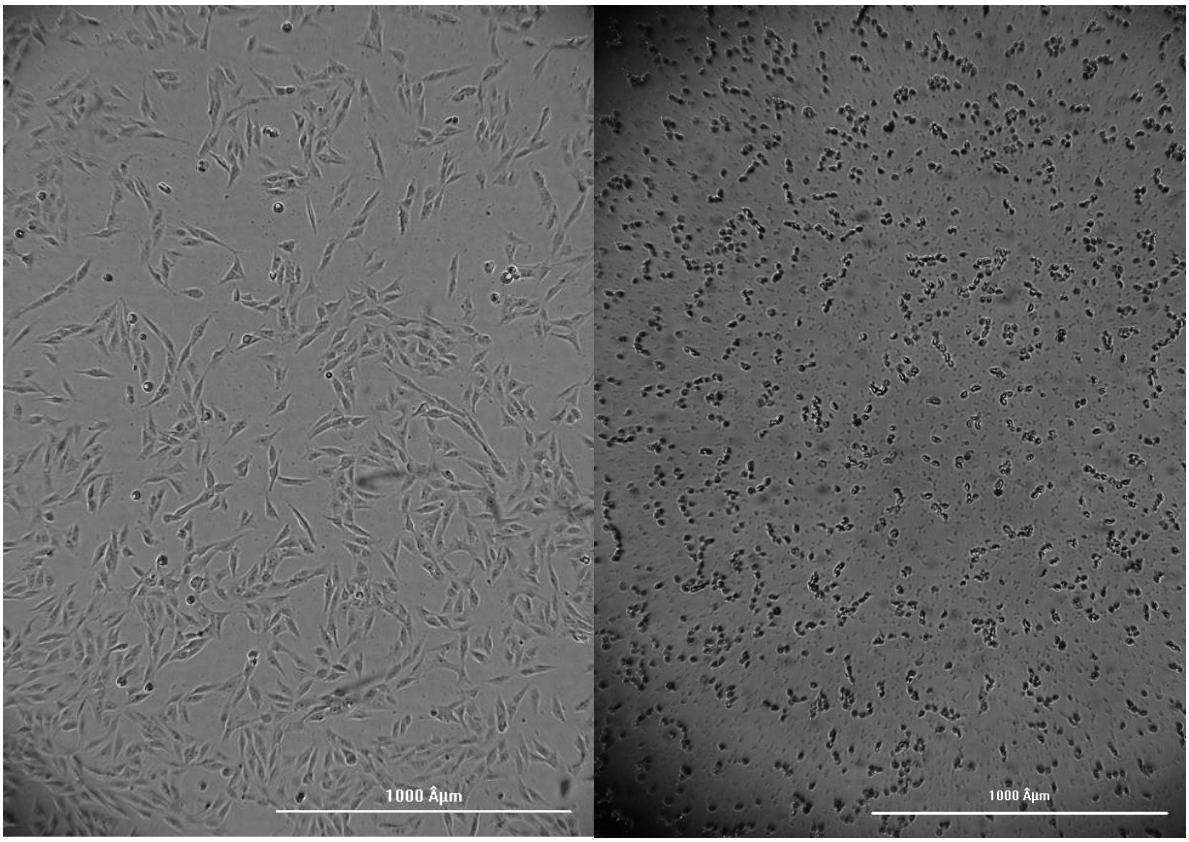

Figure 1: 2D viability assay on cancerous MG-63 cells:
Left: living cells, before treatment with nanoparticles. Right: mostly dead cells, 72 hours after treatment with nanoparticles made of Palbociclib (70%) and Sorafenib (30%) (with DADO as a stabilizer)

(9)

Cardiovascular Ultrasound Imaging Using Agar Phantom

Anna Yolin[1], Aseel Nama[1], Omri Adler[1], Oscar Lichtenstein [1], Dan Adam [1]

[1] Faculty of Biomedical Engineering, Technion - IIT, Haifa, Israel

Introduction: Coronary Artery Disease (CAD), a leading cause of morbidity and mortality in the world, in generally caused by the reduction of blood flow to the heart muscle due to build-up of plaque in the arteries of the heart. Current treatments and diagnostic methods are mostly inaccurate and invasive, therefore causing complications and endangering patients. Development of noninvasive and high-resolution imaging technology can help in early diagnosis and prevention CAD.

Methods: In order to develop a high-resolution ultrasound imaging technique, we built a model of a physical system (phantom) that optimally resembles natural tissue containing small blood vessels at different distances. The phantom consisted of agar (5% concentration) that chosen as tissue mimicking material and a large central tube from which came out small tubes (diameter of 200µm).

ultrasound imaging was performed with a linear array transducer, second harmonics (Transmit at 4 MHz and receive at 8 MHz), using B-MODE imaging method (2D). Videos of 30 seconds each, were recorded, from different parts of the phantom at different shooting angles (of the transducer). Imaging each part / angle consisted of three steps: flowing water through the tubes to ensure proper flow (no blockages), then flowing a contrast agent at a concentration of 0.04% / 0.2% through the tubes, and finally, pulling out the tubes and flowing a contrast agent at the same concentration, through the spaces left in the agar.

Using classic image processing methods that include: noise filtering, resolution improvement, extraction of specific information from the image which will help us in measuring the flow characteristics and the tubes diameter. Using advanced image processing methods: super-resolution and developing new ones.

Results: Through extensive planning and preliminary experiments, we were able to create an agar-based phantom with a stable and uniform texture, without air bubbles (thanks to the use of a vacuum machine in the solidification phase). It can be used to perform a successful ultrasound imaging which will be used to improve basic and advanced resolution.

Conclusions: Development of noninvasive and high-resolution imaging technology may be possible. However, much more research needs to be done, both in vitro and in vivo. We have shown that by improving the resolution it is possible to separate close tubes and estimate their diameter. In this way it may be possible to identify vulnerable blood vessels in the cardiovascular system, treat and prevent the development of CAD. Furthermore, the

possibility to predict the onset of CAD may also give insight into the pathophysiological mechanism of the disease.

Keywords: Coronary Artery Disease (CAD), Super-Resolution, Ultrasound Phantom, Contrast Agent.

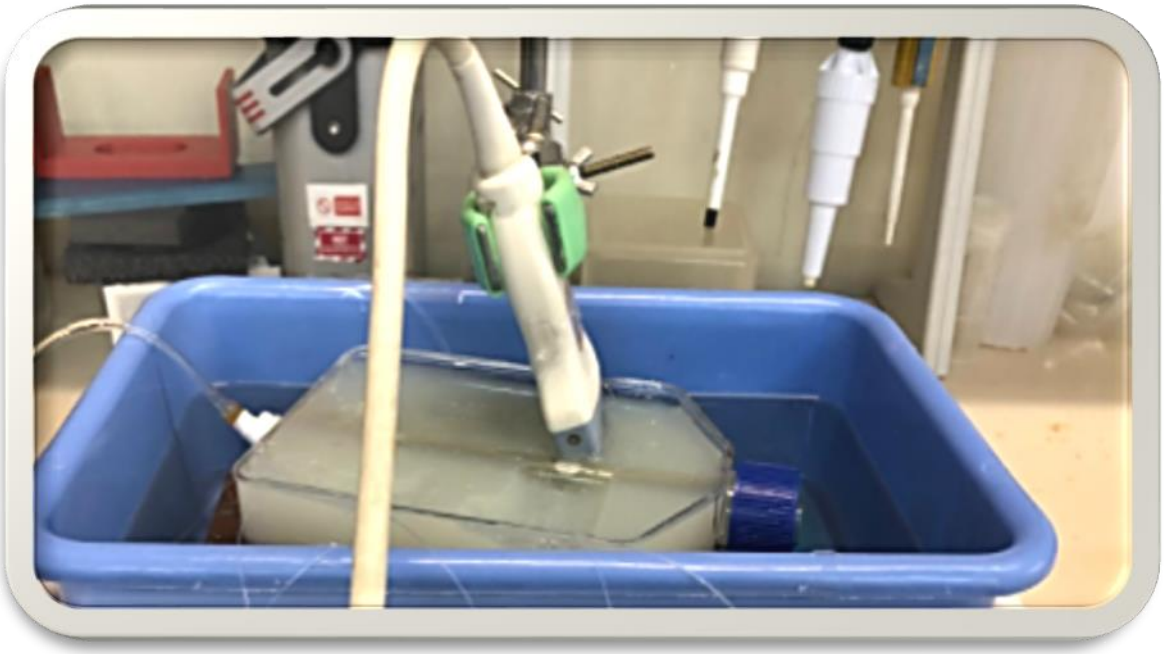

Figure 1: Experimental system – Agar phantom. ultrasound imaging performed with a linear array transducer, second harmonics (Transmit at 4 MHz and receive at 8 MHz), using B-MODE imaging method (2D).

(10)

Parent-Child Speech Synchrony During a Social Interaction

Fatima Abbas[1], Asrar Khaldey[1], Michal Zivan [2], Tzipi Horowitz-Kraus[1,2]

[1] Faculty of Biomedical Engineering, Technion - IIT, Haifa, Israel
[2] Faculty of Education in Science and Technology, Technion - IIT, Haifa, Israel

Introduction: Parent-child interaction is a topic that has been extensively researched in the field of developmental psychology. Previous studies have shown that the good interaction between parent-child affects the learning and social development of the child from infancy. Dialogic Reading- a dialogue with the child during storytelling, was found to be related to a better acquisition of language and attention skills among children. Parent-child synchronization is a key feature of interactions between them; the synchrony level represents the quality of interaction by providing a quantitative and continuous description of the interaction. However, it is still unknown how dialogic reading effects related to the level of parent-child voice synchronization. This study aims to build an automated system in order to answer this question.

Methods: The project was based on 10 pairs of Arabic-speaking mothers and their children (4-7 years old), the data included records of dialogic story-reading interaction at home (3-5 records a week for 4 weeks). A set of behavioral tests were conducted before and after intervention. The data analysis was performed by an automated system witch separate the mother and child voices using Voice-Type-Classifier algorithm, extracting the voice properties (Pitch, Intensity, Speech Rate and Ping-Pong) of the mother and the child using MATLAB and ALICE algorithm. Thereafter, a correlation analysis was preformed to study the relationship between mother's and child's voice properties during the dialogic reading, the voice properties has been tracked over the intervention in order to evaluate improvement in mother-child speech synchrony. Finally, a statistical analysis was performed to find a relationship between the behavioral tests scores, which was tested at last year's project, and the automatic system's results.

Results: The mother-child voice separation system (Voice-Type-Classifier) showed a level of reliability of about 95% according to the confusion matrix. results showed that 3 pairs of participants had a positive relationship between the session number and correlation of all the voice properties (Pitch, Intensity, Speech Rate and Ping-Pong) between mother and child, 4 pairs showed a positive relationship for 3 out of 4 properties, and the rest pairs showed a positive relationship with less than 2 out of 4 properties. Moreover, the children with higher improvement in behavioral tests scores (before and after the intervention), showed higher improvement (at first and last session) in correlation coefficient between mother and child voice properties (at least for 3 out of 4 voice properties). Sessions with higher

number of dialogs (Ping-Pong) showed higher correlation coefficient between mother and child voice properties.

Conclusions: Our findings show high levels of speech synchrony accounting for different speech properties during the dialogic reading interaction. In addition, better improvement of synchrony among mother-child pairs was obtained among children with higher improvement in behavioral tests. Higher synchrony (correlation between mother-child voice properties) was observed in sessions with more dialogs (Ping-Pongs). Moreover, according to the confusion matrix, the voice separation system is reliable.

Keywords: Parent-child Interaction, Synchrony, Dialogic Reading, Speech Analysis.

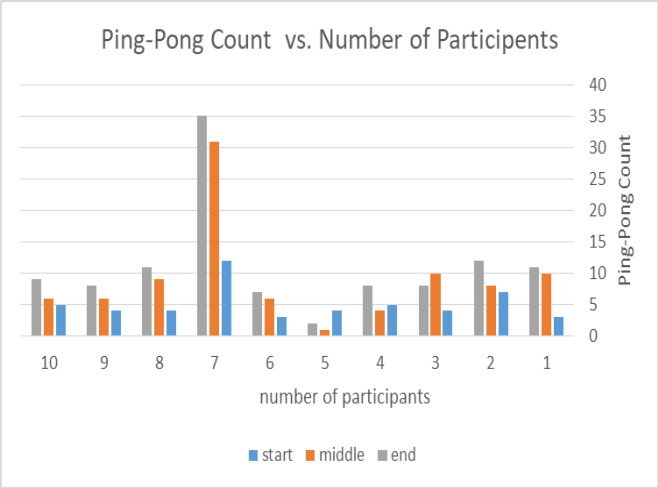

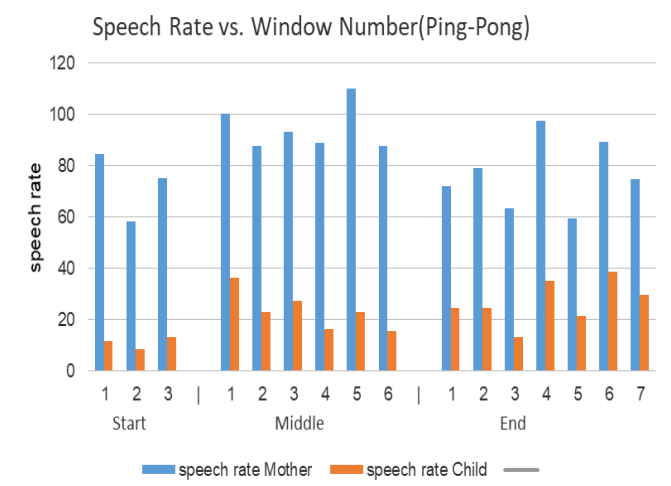

		Actual Results	
		Mother	Child
Model Predictions	Mother	TP 95.191166%	FP 4.790208%
	Child	FN 6.057875%	TN 93.941125%

Sensitivity = TP/(TP+FN) =0.9401

Specificity = TN/(TN+FP)=0.9522

Figure 1 –(A) Ping-Pong statistics over 3 time points for the 10 pairs. (B) three time points from one pair (start-middle-end) : for each time point, number of dialog windows (Ping-Pong)were calculated as shown in X axis. And for each dialog window, mean speech rate was calculated for mother and child individually as shown in Y axis. (C) Confusion Matrix for the voice separation system

(11)

Brain Tumor Segmentation using Deep Learning Methods

Hadas Ben Atya[1], Ori Rajchert[1], Dr. Moti Freiman[2]
[1]Faculty of Biomedical Engineering, Technion - IIT, Haifa, Israel
[2]Technion Computational MRI Lab (TCML), Technion - IIT, Haifa, Israel

Introduction:

Brain tumor segmentation is an important task in medical image processing. Segmentation of the tumor and its sub regions allows to assess the severity of the disease and to predict the development of the tumor.

In addition, automatic brain tumors segmentation from multi-modalities MRI is highly important for accurate reproducible measurement of tumors. Early diagnosis of brain tumors plays an important role in improving treatment possibilities and increases the survival rate of patients.

Nowadays neural networks are the state of the art of automatic segmentation in many fields, especially the encoder-decoder architectures which were first introduced by the U-Net, and recently improved by the nnU-Net. These methods require large amounts of data that are not available for medical imaging tasks. Therefore, to overcome this obstacle, we applied non-distributed augmentations to increase the variety of our training dataset and increase the robustness of our model.

Methods:

Network Architecture: We trained a 3D U-Net encoder-decoder model. The model contained five downsampling operations and five upsampaling operations. Downsampling was performed with strided convolutions, and upsampling was performed with convolution transposed.

The model used Leaky ReLU non-linearity activation function and batch normalization for feature map normalization. We trained the model for 300 epochs, with input patch of size 128X128X128 and batch size equal 5.

For the loss function, we used a combination of dice loss and binary cross-entropy (BCE) and stochastic gradient descent-based optimizer.

Data augmentation: In order to increase the variety of our training dataset and increase the robustness of our model, data augmenta-tions were applied. Our baseline transforms were implemented with MONAI and included normalization of the image intensity, intensity shift and scaling, cropping the images to 1283 patch, random flipping along the z-axis and elastic deformation.

We compared the baseline model with other models which included those transforms with an addition of mixed structure regularization, shuffle pixels noise or Gaussian-noise separately.

Mixed structure regularization (MSR): We corrupted the input data by randomly adding different brain image from our training set, as described by.

Shuffle pixels noise (SPN): A random permutation of the pixels was added to images in the training set. We applied both augmentations with different magnitudes and probabilities.

Results:

We randomly split our database into a training set, validation and testing set (80%,10%,10% respectively). Our training set contains 229 images, and the validation and testing set contain 28 images each. The tumor sub-regions dice score were computed separately for each experiment and computed the mean dice, as shown in table 1. The best dice score was achieved for the MSR model, and the dice improvements were statistical significance with a p-value of 0.0022, 0.0028 for the TC, WT respectively.

Table 1: Testing Dataset Results

Augmentation Type	**Dice Score**			
	Overall Dice	***ET***	***TC***	***WT***
Baseline	0.80959 ± 0.145	0.68795 ± 0.276	0.78975 ± 0.207	0.88811 ± 0.081
Gaussian noise	0.80775 ± 0.134	0.69871 ± 0.264	0.77113 ± 0.222	0.8918 ± 0.0.06
SPN	0.81987 ± 0.16	0.70344 ± 0.285	0.79351 ± 0.24	0.89983 ± 0.094
MSR	0.82396 ± 0.156	0.69705 ± 0.287	0.80732 ± 0.234	0.90404 ± 0.08

Conclusions:

We applied several different augmentations in order to enhance the segmentation quality. We managed to achieve a statistical significant improvement using the MSR. This non-specific method improvement might be achieved in different biomedical-datasets.

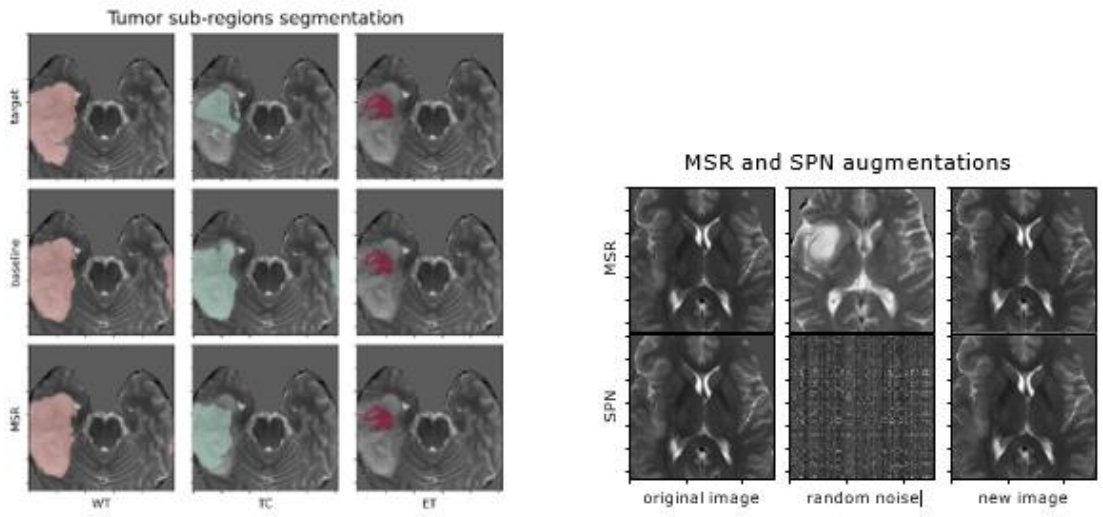

Figure 1: Left figure: Tumor segmentation with nnU-Net. Target structures are shown in 2D (first row), the baseline model's outputs (second row), and our model with mixed structure regularization - MSR outputs (third row). Right: Example for the MSR and SPN augmentations. First row: MSR augmentation, the original image was corrupted with a randomly selected new image from the dataset. The noise magnitude was set to $1e$ 4 and the probability for applying the augmentation was $p = 0.5$. Second row: SPN augmentation, the image was corrupted with a pixel shuffling in both x, y axes. The noise magnitude was set to $1e-7$ and a probability of $p = 1.0$.

(12)

Reorganization of Functional Networks Following MRI-Guided Focused Ultrasound Treatment in Essential Tremor Patients

Iyar Hadad[1], Naama Rivlin[1], Gil Zur[2], Noam Bosak[3], Firas Mawase[1]

[1] Faculty of Biomedical Engineering, Technion - IIT, Haifa, Israel
[2] Department of Radiology, Rambam Health Care Campus
[3] Department of Neurology, Rambam Health Care Campus

Introduction: Essential tremor (ET) is a progressive neurological disorder characterized by a 4-12Hz tremor in the hands or head, which occurs when performing daily activities. In the U.S alone, 7 million new patients are diagnosed each year. Significant clinical success has recently been achieved in ET treatment by ablation of the ventral intermediate nucleus (VIM) in the thalamus using Magnetic Resonance Imaging guided Focused Ultrasound (MRgFUS), resulting in immediate relief to complete elimination of the tremor. However, this treatment has side effects that varies between patients, and the neural mechanism by which the treatment succeeds in reducing or eliminating tremor is not well understood. This project presents a method for collecting and analyzing data from ET patients before and after MRgFUS treatment, aimed at gaining a better understanding of the treatment mechanism and therefore allow optimal selection of the candidates.

Methods: The experimental system consists of an MRI scanner, a tri-axial accelerometer, and MRI-compatible electromyogram (EMG) electrodes. The participants were scanned in the described system while performing a tremor-stimulating task that includes blocks of alternating hands extension and rest. EMG and functional magnetic resonance imaging (fMRI) data were collected from 2 ET patients before treatment, 1 Parkinson's patient before and after treatment, and 1 healthy adult. Participants that were found to be ineligible for treatment were not included in the trial. The EMG data was pre-processed in MATLAB to create a residual EMG (rEMG) regressor for the fMRI data. fMRI data was analyzed using Statistical Parametric Mapping software (SPM12).

Results: We were able to identify the motion blocks corresponding to the motor task in the EMG signals of all participants. We created a MATLAB program that accepts the raw EMG signals and outputs a vector containing the tremor intensity in each block, i.e., an rEMG regressor for the fMRI. Regarding the fMRI, activity in the motor areas during the task was detected for the 2 participants who have not yet undergone treatment. Post-treatment data is needed to draw conclusions. For the treated participant we were unable to detect activity in the motor areas, most likely because of bad signal quality.

Conclusions: The changes in functional connectivity in the brain before and after MRgFUS treatment have not yet been studied and using EMG recording to identify them better has a great potential. This can be seen from the signals received and the vast amount of information

they contain. However, data collection is a long process and the data we have is limited and noisy, making it difficult to draw conclusions.

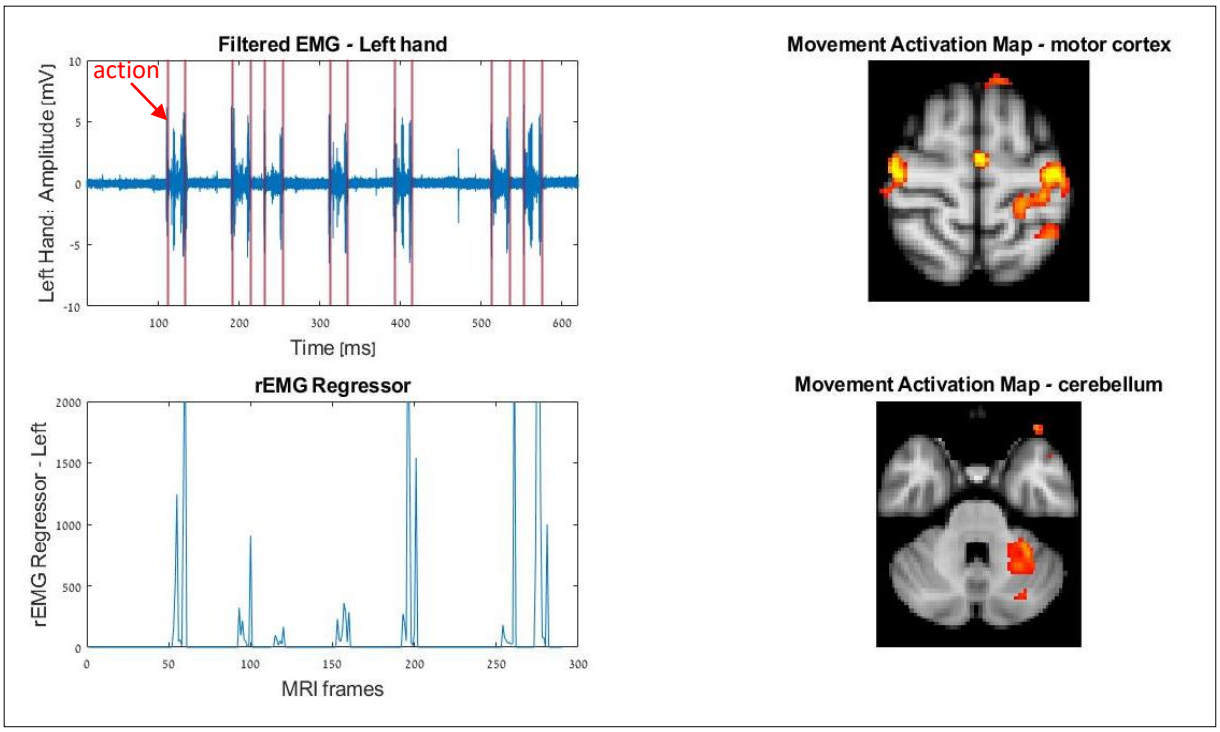

Figure 1 - At the left, EMG signal from the left hand of an ET patient using our system during a motor task (top), rEMG regressor created from the presented EMG data before convolution with canonical HRF for fMRI analysis (bottom). At the right, Activation map while performing the left action, seen in the motor cortex and the cerebellum.

(13)

AI Based Decision Support System for Labor and Delivery Management

Amit Parizat[1], Rotem Shapira[1], Noam Keidar[1,2], Joachim Behar[1], Yael Yaniv[1]

[1]Faculty of Biomedical Engineering, Technion - IIT, Haifa, Israel
[2]Faculty of Medicine, Technion - IIT, Haifa, Israel

Introduction: Labor complications are a major concern for obstetricians and their patients, potentially leading to long-term consequences for both mother and newborn, and even mortality. The risk for such complications is correlated with clinical factors like maternal background diseases, age, and obesity. Obstetricians identify complications and make fateful decisions regarding medical interventions before and during labor based on the mentioned parameters and on the cardiotocography signals. Obstetric teams' reliance upon the monitor is suboptimal since analyzing the long signals manually is challenging, yet it is a common and accepted practice. Misinterpreting the fetal monitor leads to labor complications, and to unnecessary cesarean sections as a precautionary measure to the slightest indication. Cesarean sections' rate is continuing to rise at an alarming rate to current third of all births, raising the need for a well-established, reliable tool to prevent needless invasive interventions and save lives.

Methods: First, we developed a trustworthy and robust code platform for signal processing and for training machine learning models. Second, we acquired data from the open-access dataset "CTU-CHB Intrapartum Cardiotocography Database", which contains 552 samples of the fetal heart rate and uterine contractions signals, 19 different clinical features and 6 outcome labels. We preprocessed the biological signals using popular digital signal processing methods for noise reduction, gain increase and normalization, and extracted features from the signals to optimize the analysis. Third, we used neural network models like temporal, convolutional and fully connected neural networks to classify the samples into healthy and unhealthy groups which were defined by the pH of the umbilical arterial blood sample. We tried various combinations of clinical parameters, recorded signals and extracted features with different models.

Results: As our goal is to create a decision support machine that will lead to a decrease in the number of unnecessary cesarean sections, the significant metric for assessing our work is the positive predictive value, which in the clinic is about 25%. Using clinical features only, the most successful fully connected neural network model reached 74.3% accuracy, 88.2% positive predictive value, 75% sensitivity, 72.4% specificity and 0.81 F-score. When using both features and signals, the most successful convolutional network reached 79.8% accuracy, 85.7% positive predictive value, 80.6% sensitivity, 78.6% specificity and 0.831 F-score.

Conclusions: Creating a prediction system of obstetric complications during childbirth is feasible, and it could be effective and useful for the decision-making process of obstetricians. We believe that training the models on more extensive databases would enhance the prediction ability of this system facilitating improvement of obstetric outcomes.

Keywords: electrical fetal monitor; perinatal asphyxia; neural networks; cardiotocography.

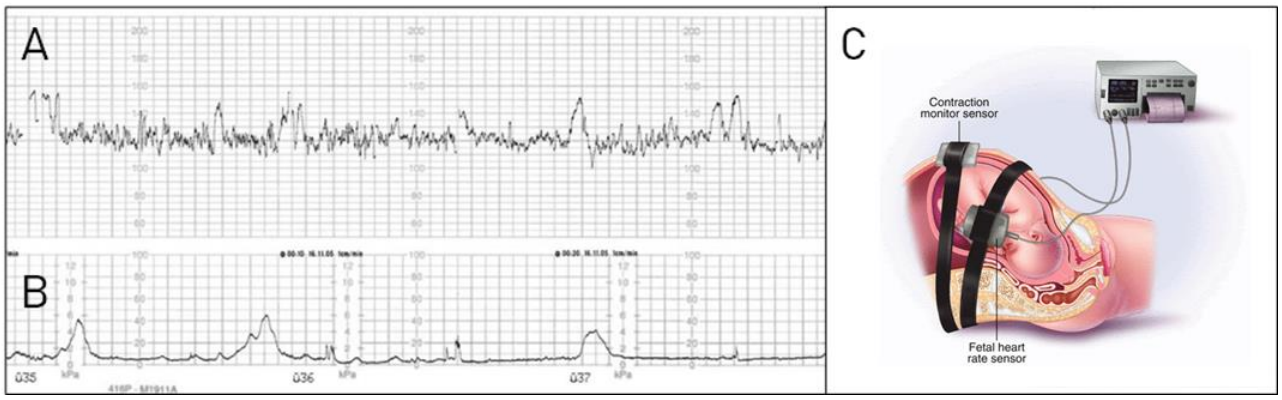

Figure 1 - Electrical fetal monitor, sensor placement and routinely recorded signals. (A) Fetal heart rate signal, (B) Uterine contractions singal, (C) Monitor usage and sensor placement illustration.

(14)

Optimizing Immune Cell Tracking Methods for Multimodality Imaging

Sivan Barash[1], Shachar Zigron[1], Moti Freiman[1], Katrien Vandoorne[1]

[1] Faculty of Biomedical Engineering, Technion - IIT, Haifa, Israel

Introduction: Diseases of the cardiovascular system are the leading cause of death in the world.
Although cardiovascular disease has been classically thought of as a lipid storage disease, it has become clear that one of the main drivers is inflammation, in which monocytes and macrophages have a major role. The mechanisms of in vivo macrophage dynamics causing disease are unclear. Therefore, a better understanding of macrophage functions and dynamics in pathogenesis will open new opportunities for better diagnosis, prognostic assessment, and therapeutic intervention. Accurate, non-invasive real-time cell-tracking by imaging tools of extensive recruitment of macrophages to inflammatory sites can answer important questions regarding their dynamic roles and behavior in stable condition and in heart disease. To improve the methods currently being researched today of tracking macrophages (that has not been introduced into clinical practice) and provide the basis for in vivo tracking, we aimed to optimize labeling strategies and define sensitivity of macrophage in multimodal imaging (MRI, IVIS).

Methods: First, we cultured RAW 264.7 macrophages cells. Cell viability was examined by Trypan-Blue and characteristic round morphology observed under the microscope. Next, agarose (2%) gel phantoms of 100µL were prepared with variable numbers of cells $(5, 10, 25, 50, 100 \cdot 10^3)$ labeled either with RhoB-BSA-GdDTPA, or with Cy647-Dextran-CLIO. Cellular uptake of both contrast agents was verified by fluorescent microscopy. The cells were imaged by preclinical 9.4T Bruker Biospin MRI using multi-slice multi echo (MSME) with 10 variable echo times for T2 mapping and using a gradient echo with 15 variable repetition times for T1 mapping. In addition, IVIS imaging was performed on the prepared phantom with different concentrations of cells to measure the fluorescent signal from the labeling cells. Analysis was performed on T1 and T2 maps, their fitting curves and ROI values, that were obtained by MATLAB.

Results: On microscopic images we were able to verify uptake of both labels by the macrophages. Next upon MR imaging, the decrease in T2 values of cells labeled with Dextran-CLIO compared to the T2 values of not labeled cells (36-65%) was greater than the decrease in T1 values of cells labeled with BSA-GdDTPA (4-33%). In relation to control group (unlabeled cells), T1 and T2 were shorter in any examined cells amount. Upon IVIS imaging, as the cell concentration increased, a higher fluorescent signal was obtained.

The T1 and T2 values are summarized in Table 1:

Labeling	Cells number $(*10^3)$	T1 [ms]	T2 [ms]
Not labeled	50	2355.05	93.18
BSA-GdDTPA	5	2301.01	-
	10	2168.26	-
	25	2046.92	-
	50	1756.03	-
	100	1614.32	-
Dextran-CLIO	5	-	59.5
	10	-	57.74
	25	-	49.24
	50	-	36.59
	100	-	33.07

Conclusions: For maximal signal obtaining from macrophage cells in MRI, labelling with Dextran-CLIO particles was better internalized by macrophages, as opposed to labelling with BSA-GdDTPA, we can conclude that it is the preferred labelling method. For in vivo tracking, 5,000 cells in 100 μL solution is about the amount that will be recruited to the inflammatory site and is sufficient for detection in MRI or IVIS. In case of higher required signal (higher background for example), a larger number of cells can be labeled and eventually detected. This study could initiate future research to translate quantitative macrophage imaging towards in vivo preclinical imaging.

Keywords: Cell tracking; Macrophages; MRI; Cell imaging; Cell labeling.

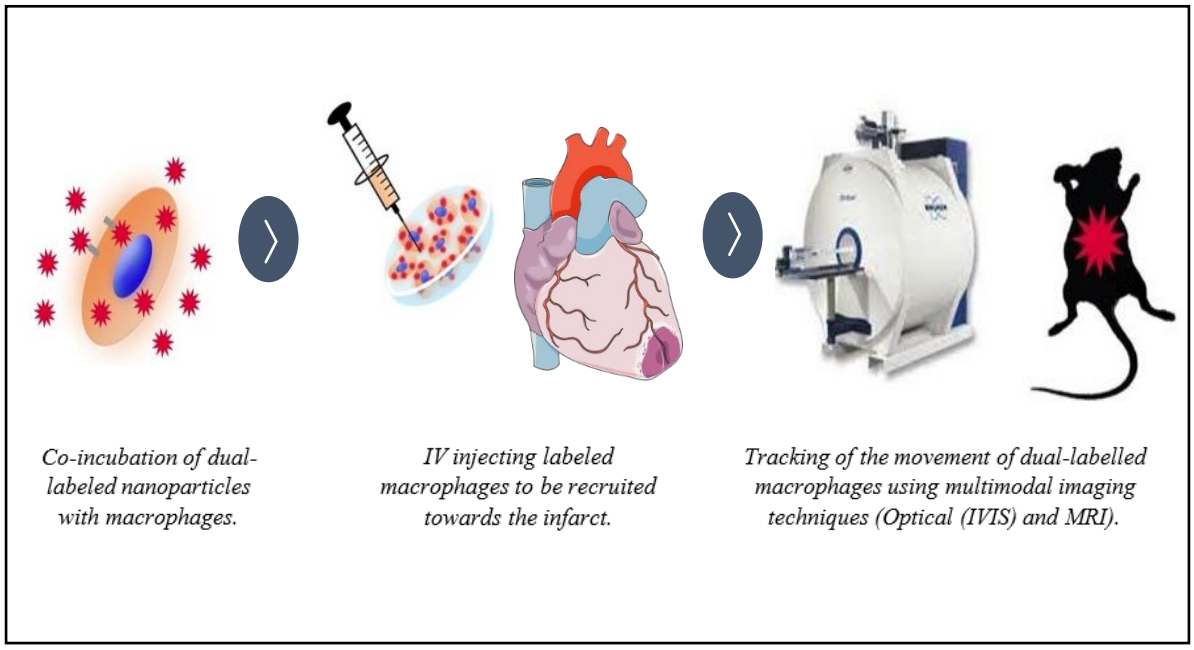

Figure 2: Current and future research flow chart

(15)

Identification of Candidate Chronotherapeutic Drugs Through Their Molecular Targets

Ofek Aloush[1], Shahaf Karpenkop[1,2], Jonathan Sobel[1], Joachim Behar[1]

[1]Faculty of Biomedical Engineering, Technion - IIT, Haifa, Israel
[2]Faculty of Medicine, Technion - IIT, Haifa, Israel

Introduction: Chronotherapeutic refers to a treatment method in which drug availability is matched to physiological rhythms, to optimize therapeutic outcomes. Circadian genes are oscillators that cycle with a near-24h period, a stable phase and may be synchronized by external cues (i.e. day-night cycle, feeding-fasting). circadian rhythms are linked to different pathologies, for example, some cardiovascular diseases like paroxysmal atrial fibrillation have a higher occurrence during the morning time, due to the uprise in provoking factors, like the elevation of blood pressure and certain hormones. Approximately 50% of current drugs target the product of a circadian gene and the efficiency of a drug often substantially depends on the time of administration. However, orders for therapies, are commonly placed during rounds or thereafter, regardless of the circadian biology that might be involved. Although the chronotherapeutic approach is more widely acknowledged as beneficial, it is still not comprehensively used.

Methods: The first step was analyzing gene expression datasets to find oscillating genes. The analysis was made with gold-standard algorithms and a sequential neural network designed by us. The data set is comprised of a baboon's heart tissue RNA-seq, harvested every 2 hours to create a diurnal gene expression profile. further pathway analysis was made with Enricher gene enrichment analysis tool and Cytoscape to explore gene functions. The second step was analyzing the DrugBank database and identifying drugs targeting genes that were classified as circadian. Mechanism of drug action, absorption time, half-life, and a drug indication "text mining" were used and explored to recommend an optimal dosing schedule.

Results: 3,036 out of 18,596 (16%) heart genes were classified by our model as circadian; their amplitude and phase were calculated, and a 24-hour gene profile was plotted. After comparing the results to the drug database, 1,487 drugs were found to target, be transported, or be modified by a circadian gene product, and 1613 out of the 3,036 heart circadian genes were targeted by a drug. We explored each drug by clinical relevancy, biological mechanism, and the target circadian profile. We suggest a list of 5 drugs for treating – atrial fibrillation, arrhythmia, and myocardial infraction, that we classified to have high potential to benefit from an improved chronotherapeutics approach dosing schedule. Finally, a schedule as such was proposed for each drug.

Conclusions: many common clinical cardiovascular drugs target or are affected by a circadian gene product, and the chronotherapy approach may be beneficial in lowering mortality rates and reducing adverse effects, length of hospitalization, and treatment costs, yet further

validation (pre-clinical or clinical) is necessary to validate our proposed schedules. Furthermore, success in improving treatment outcomes might emphasize the benefits of the chronotherapeutics approach in other diseases, leading to better treatment and improved patient life quality.

Keywords: chronotherapy, circadian genes, cardiovascular diseases, data mining and neural networks.

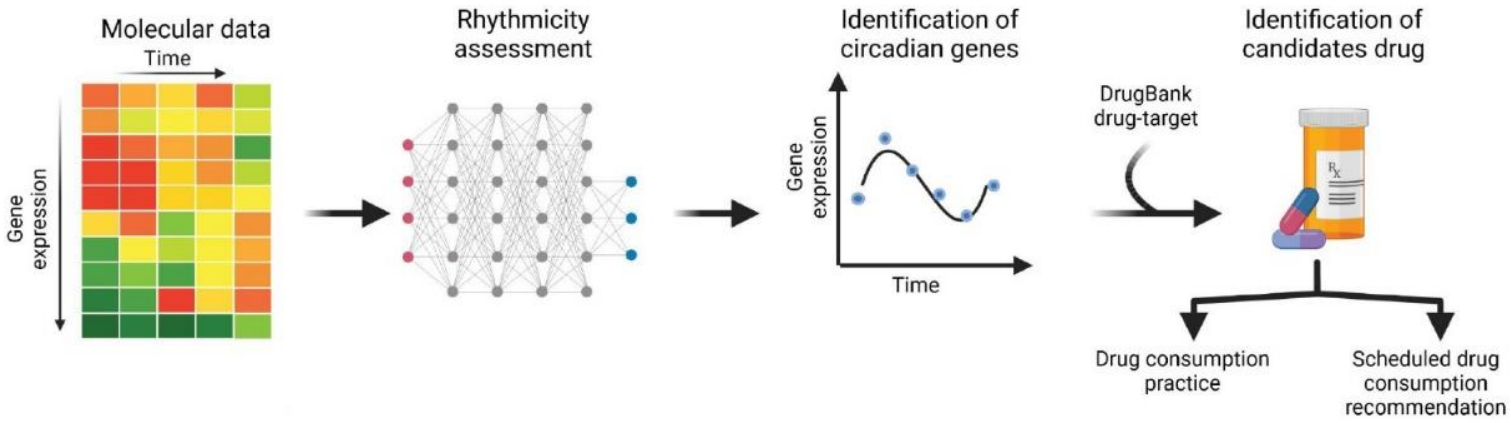

Figure: Project flow

(16)

Characterization of Cell Assembly and Electrophysiological Properties in Engineered Heart Slices

Lior Haim[1,2 *], Nir Litver[1,2 *], Arbel Artzi Schnirman[1], Matteo Ghiringhelli[2], and Lior Gepstein[2]

[1] Faculty of Biomedical Engineering, Technion - IIT, Haifa, Israel
[2] Ruth and Bruce Rappaport Faculty of Medicine, Technion - IIT, Haifa, Israel
[*] equal contributors

Introduction: Engineered cardiac tissues are currently used in medical research to study arrhythmias, congenital heart diseases, drug testing, and more. One particular technique for the creation of engineered heart tissue is known as engineered heart slices (EHS), which are made out of decellularized extracellular matrix (dECM) as a scaffold and induced pluripotent stem cells derived cardiomyocytes (iPSC-CMs). However, the manner in which the structure of the scaffold affects the spatial organization of the seeded cells was not yet thoroughly investigated.

Methods: We created EHS using a decellularized porcine heart slices, which we had previously frozen and cut using a cryotome, and cardiomyocytes which were differentiated from iPSCs and cultured at 37°C and 5% CO_2 with RPMI medium. After decellularization using temperature and chemicals treatments we dissociated the cells, seeded them on the ECM sheets and let them air-dry to allow maximal adhesion. The EHS were later fed with RPMI medium and cultured at the incubator. We assessed the tissue properties using live-imaging, antibody staining for collagen, actinin and vimentin, and electrical mapping of the action potential.

Results: In well-seeded EHS constituted of well-differentiated cardiomyocytes, we observed a correlation between the cell orientation and the collagen fibers in the EHS. In these EHS, the action potential propagation (shown in figure 1) and tissue contractility matched the structure of the EHS. In other cases, cells tended to create aggregates and did not assemble in the direction of the ECM fibers due to poor differentiation.

Conclusions: Since the direction of mechanical contractility and the propagation of AP in derived of cell orientation, well-differentiation is the key to a well-functioning tissue in which the cells are align with the orientation of the ECM. In these cases, the contractility and conduction will be derived from the ECM fibers.

Keywords: EHS, Tissue Engineering, Cardiac Tissue, Cardiac electrophysiology

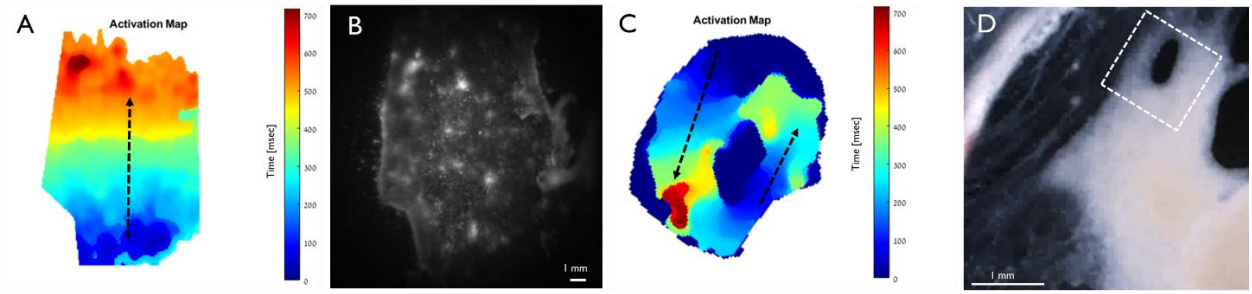

Figure 3: (A) Activation map showing voltage distribution throughout the EHS. Arrows indicating AP propagation direction, analyzed using nameofsoftware. (B) The same area of interest shown from the live imaging. (C) Activation map showing a bi-focal AP propagation , analyzed using nameofsoftware. (D) Same area of interest from live imaging, ROI is marked in white square.

(17)

Plasticity of Synapses in Zebrafish Larvae due to Epileptic Seizures

Avigail Berger[1,2], Noya Zeret[1,2], Ory Perelsman[1], and Limor Friefeld[1]

[1] Faculty of Biomedical Engineering, Technion, Haifa, Israel
[2] Faculty of Medicine, Technion, Haifa, Israel

Introduction: Studies show that epileptic seizures appear when there is an imbalance between excitatory neurons and inhibitory neurons. Many genetic epilepsy syndromes are caused by mutations affecting synaptic function and in particular the function of inhibitory synapses. Moreover, some studies show that there is a connection between epileptic episodes and receptor cluster changes without a genetic background. Therefore, we aimed to test whether epileptic seizures can cause changes in the clustering of inhibitory receptors, in particular glycine receptors (GlyR). While testing this hypothesis, we used expansion microscopy (ExM) – a method used in the Friefeld lab in which we expand and fix biological samples to allow imaging with better resolution. The method includes embedding the sample in a delicate and brittle gel that is hard to handle under the microscope, while imaging only in a specific orientation. Therefore, another aim for our project is to optimize a re-embedding protocol to create a new, more resilient gel that will allow the researcher to view the sample in three dimensions under the microscope.

Methods: We used zebrafish larvae as our model – we divided 5 dpf larvae into three groups, each group placed in a different medium for an hour: breeding water (control), strychnine (for validation of the process) and bicuculline group (experiment group). We then dissected the brains, stained them and embedded them in gels, then expanded the gels for an improved resolution and re-embedded them with a different protocol for a more resilient gel. Next, we imaged samples using a spinning disk confocal microscope. We repeated this process in three different iterations for better statistical power.

Results: In each iteration, we managed to expand the samples by a factor of four isometrically (as expected). In most samples, after re-embedding, the signal was slightly weaker especially when we changed the protocol to create an even stronger gel. Regarding the density of the GlyR clustering, it seems that the receptors on cells from the experimental group are slightly more dense then those of the control.

Conclusions: Our goal was to adapt the existing re-embedding protocol in a way that will allow the user to view the sample in three dimensions with minimal damage to the sample. In our project, we managed to load the re-embedded gel onto a fep tube to image the same sample in different directions under a confocal microscope. Thus, we showed that it is feasible to create a finished protocol that will allow easier handling of delicate samples. Regarding the receptor

clusters, results show that epileptic seizures might cause plasticity in the synaptic structure, although further analysis and research are needed.

Keywords: Epilepsy; Receptor clustering; Expansion microscopy; Gel re-embedding.

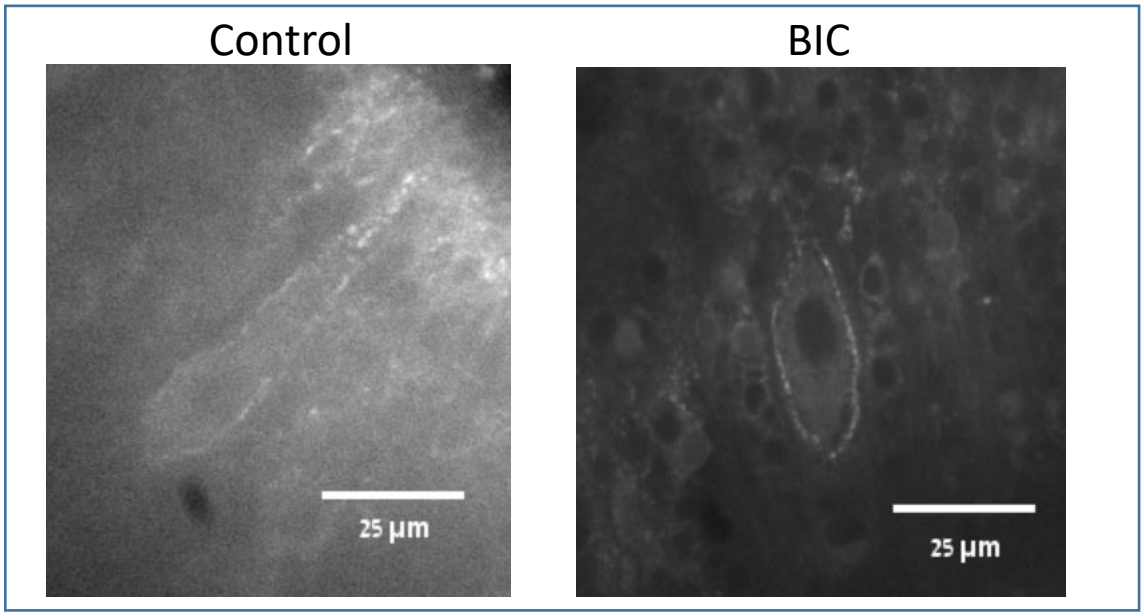

Samples in agarose (pre-expansion). Staining: primary – mouse anti-GlyR, secondary – Atto 647 anti-mouse. This figure demonstrates the differences in the receptor clustering between the groups.

(18)

Predictive Model for Core Temperature from Thermal Face Images

Avraham Tenenbaum[1,2], Sivan Geva[1,2], Nati Daniel [2], Yonatan Savir[2]

[1] Biomedical Engineering Faculty, Technion - IIT, Haifa, Israel
[2] Faculty of Medicine, Technion - IIT, Haifa, Israel

Introduction:

Body temperature is a basic indicator of people's health. Infrared (IR) thermography is a safe, non-invasive, and low-cost technique for measuring body temperature. InfraRed detectors are widely used nowadays, especially due to COVID-19, for skin temperature measurement. An immediate advantage of IR detectors is a safe measurement without exposure to virulence factors of the patient. Moreover, IR detectors can assist in real-time hospitalization monitoring, and so, aid to adjust patient's treatment in real-time, thus, reducing deteriorations and complications.

Methods: We designed a pipeline of image processing followed by a deep learning model. For the image processing task, we preprocessed a dataset of thermal videos (300-400 frames each) from "Belinson" Hospital, E.R patients (n = 253). The preprocessing contained manual crude body cropping, auto face recognition and ellipse cropping using HaarCascade algorithm, excluding background using Otsu algorithm, normalizing each image to a black-box temperature sensor. For the deep learning task, we designed a feature extraction models followed by a supervised learning classifier/regressor. We used two different feature extraction models: CNN consisting of VGG16 concatenating to NetVLAD, representing each thermal image as a vector of 4096 parameters. The second is based on CNN resnet101 backbone, representing each thermal image as a vector of 2048 parameters. Next, Multilayer perceptron (MLP) classifier and regressor were trained on the vectors extracted from both models.

Results: For core temperature detection, the best MLP classifier model received best score using NetVLAD model with a score of 57%.

The scores from both models are summarized in Table 1:

Feature extraction model	Accuracy
NetVLAD	50-60 %
ResNet101	50-60 %

Conclusions: Both models gave poor prediction rate of the patient's core temperature. However, deep encoders showed a clear visual (on PCA and TSNE), separation between subjects, suggesting that the vectors features are unique and the connection to temperature is not clear due to lack of data. Therefore, we believe enlarging dataset quantity, increase in size and in patient's temperature variability as well as improve dataset quality, reduction of noise will improve results significantly.

Keywords: InfraRed detectors; Deep Learning; NetVLAD; Resnet101, Feature Extraction.

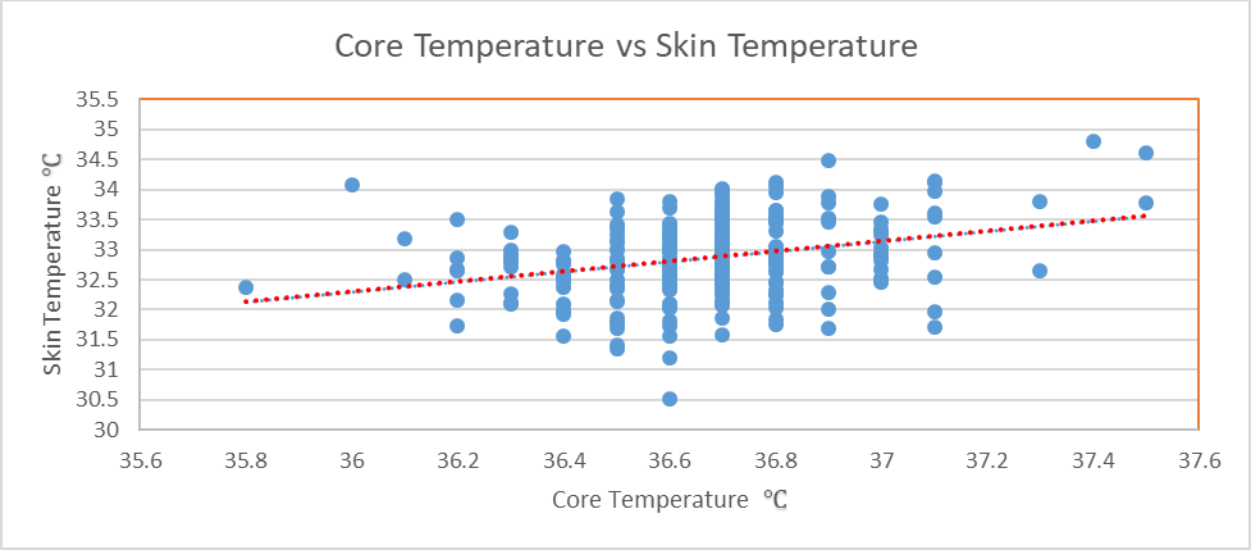

Figure 1: Raw data scatter plot- core temperature vs average face skin temperature, per patient.
Project Motivation- The progressed trendline shows a positive correlation between core temperature and skin temperature.

(19)

HRV-CAM: A Novel Approach for Remote Detection of Cardiac Arrhythmias

Yonathan Belicha[1], Daniel Cherniavsky[1], Moran Davoodi[1], Joachim Behar[1], Yael Yaniv[1]

[1]Faculty of Biomedical Engineering, Technion - IIT, Haifa, Israel

Introduction: Cardiac arrhythmias are abnormal conditions of the heart that are associated with its' electrical conduction system and mainly characterized with irregularity of heartbeats. Arrhythmias can lead to heart failure, stroke and even sudden cardiac arrest. The gold standard clinical method used these days to diagnose these disorders commit the presence of the patient in the nearby healthcare campus. It also requires physical contact with a medical device, mostly ECG. Heart rate variability (HRV) is a set of statistical measures of the heartbeats regularity that can be beneficial for arrhythmias detection. We propose a novel approach to detect these conditions by HRV measured remotely using short videos monitoring a patient. The videos can be acquired by a smart phone and by that save significant amount of time, expanses and in some cases even lives.

Methods: We created a system consists of two parts:

- Remote HRV measurement platform.
- Detection algorithm based on machine learning model.

First, we used an existing method to extract heart pulsations from pixel values variations in recorded video of human skin surfaces. This method is based on amplifying minimal color variations in the face that is correlated to the cardiac cycle. Afterwards, to find accurate beat-to-beat signal, we processed this output signal by Butterworth filter and located the heartbeats by mathematical tools and physiological priors. In order to analyze our signals, we have transformed them to HRV features by using PhysioZoo platform.

Then, we trained a machine-learning model, which is based on 750 ECG time windows recordings from MIT-BIH published in Physionet. The database consists of 18 normal sinus rhythm subjects and 7 atrioventricular block (AV block) subjects. We looked for the ideal time window length that will be the shortest yet informative enough. Ideal window length was 1 [min]. Moreover, we used statistical tools to reduce the dimensionality of our features to create a compact and yet reliable model. The output of our model is a soft assignment of the features, i.e. it calculates the probability that an AV block event had occurred in the current time window.

Results:

- Our remotely extracted signal is comparable to beat-to-beat ground truth signal extracted from Photoplethysmograph (PPG) up to an error of $[4.98\% \pm 1.37\%]$.
- For AV block detection based on ECG recordings we achieved the following performances:
  Sensitivity – 86%, Specificity – 99%, PPV – 97%, NPV – 96%, AUC – 99%.
- For remote AV block detection, we achieved:
  Sensitivity – 100%, Specificity – 89%, PPV 50%, NPV – 100%, AUC - 94%.

Conclusions: HRV contains valuable information even in a relatively short time window. This kind of information can be used to diagnose conduction disorders. Moreover, we are suggesting a remote tool that can reliably extract beat-to-beat signal, calculate HRV from it and detect AV block. This kind of tool opens a wide range of possibilities in the field of digital healthcare era.

Keywords: Conduction Disorders; Heart Rate Variability; Remote Medicine

(20)

Compact Spectrally Encoded Interferometry Probe for Imaging the Acoustic Reflex in Humans

Chen Berkovich[1], Rahel Rosen[1], Lidan Fridman[1], Matan Hamra[1], Dvir Yelin[1]

[1]Faculty of Biomedical Engineering, Technion – IIT, Haifa, Israel

Introduction:

The acoustic reflex is an involuntary contraction of the stapedius muscle in the middle ear, induced by high intensity sound. This mechanism pulls the tympanic membrane in and reduces transmission of sound to protect the sensitive structures of the inner ear. The reflex is affected by mechanical changes in sound transmission, and its neurological pathway includes the VIIIth cranial nerve, the cochlear nucleus and the brainstem. Therefore, the information obtained can be used clinically to define middle ear, cochlear, and VIIIth-nerve disorders, and is a fundamental factor in performing hearing tests and achieving a correct diagnose.

Traditionally, the reflex threshold is measured by tympanometry methods which include pressure-sealing the ear and measuring the intensity of reflected sound of different frequencies (probe tone), while activating the reflex with another high intensity sound (pure tone). This could be inaccurate and has significant variance.

Interferometric spectrally encoded endoscopy (ISEE) has been shown capable of high-speed imaging of nanometer-scale vibrations of the tympanic membrane in human subjects. In this project, we design an alternative test for the acoustic reflex threshold measurement using ISEE imaging of real-time movement of the tympanic membrane. This should allow for a simple, easy to use and more accurate test, and provide additional data that is not available to physicians today. Integrating this test into the system will enable performing several complementary tests using a single device.

Methods:

ISEE measures the spectral interference between a reference beam and spectrally encoded reflections from the target tissue. Under acoustic stimulations, the axial tissue motion induces wavelength-dependent phase shifts that are captured by the high-speed spectrometer. By slowly scanning the imaging line across the tissue, the full vibration pattern is recovered at high lateral resolution and nanometric axial sensitivity.

Analyzing those results to measure the change in the acoustic immittance in the ear canal, caused by a high intensity sound, enable to determine:

- Presence or absence of the acoustic reflex.
- The acoustic reflex threshold.
- Acoustic reflex decay (if tested).

Results:

The test requirements and current implementation were characterized, and a full measurement protocol was designed, including stimuli and sound calibration. This was integrated into the existing ISEE system.

The algorithm was iteratively optimized for processing time and got reduced by 60%, allowing near real-time imaging and a more accurate result. First feasibility testing showed valid results in humans.

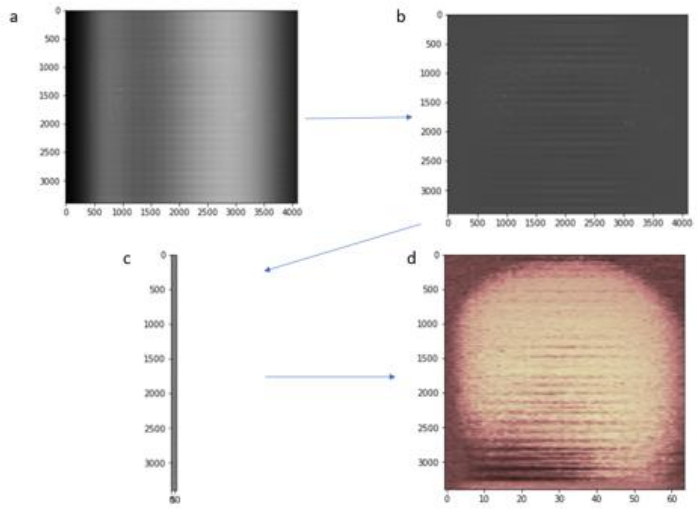

Figure 1: image processing.
a. Raw data produced from line camera **b.** matrix after detrending **c.** phase shift vector, calculated using $\mathcal{H}\{\}$ Hilbert transform **d.** final image, vibration map of the tympanic membrane at a given time

Conclusions:

A full testing protocol and system were characterized and designed for real-time *in vivo* measurement of the acoustic reflex threshold in patients. Future work will include feasibility tests in human volunteers comparing to current gold-standard, and further analysis of additional data acquired.

Keywords: interferometric spectrally encoded endoscopy (ISEE), acoustic reflex, tympanic membrane, hearing problems, clinical diagnosis

(21)

The effects on uncertainty and frequency of movements on their representation in the motor cortex: a TMS study

Matitiahu Gorodetsky[1], Marvyn Bebar[1], Abed Suleiman[1], Firas Mawase[1]

Biomedical Engineering Faculty, Technion - IIT, Haifa, Israel

Introduction: It has been established that action selection and execution, is influenced not only by current state of our body and the environment, but also by the recent history of our movements. The hallmark of this form of change is called use-dependent plasticity (UDP) and can be thought as directional biases of movement toward previous repeated direction. Two forms of such UDP effect have been observed in previous studies: (1) TMS biases - in which repeating simple thumb movements (i.e., training) toward a particular direction subsequently led to a dramatic influence on involuntary movements elicited by cortical transcranial magnetic stimulation (TMS). (2) Movement biases - in which repeating movement in one direction during pure behavior paradigms lead to directional biases toward the repeated direction when reaching to adjacent targets. Nevertheless, the dissociation between directional biases in TMS paradigms (TMS biases) from biases that arise in pure behavior paradigms (movement biases), as in reaching movements, has never been addressed. The aim of the current project is to determine whether directional biases observed in TMS paradigms (TMS biases) are distinguished from biases arising from pure behavior paradigms (movement biases), by systematically dissociating them.

Methods: Subjects were seated comfortably in a chair with their right forearm immobilized to the table while their thumb is free to move. While subjects (n=5) are seated a head simulation using TMS was preformed to determine the TMS-evoked thumb movement default angle. Subjects were studied using different thumb voluntary movement experiments, to evaluate their baseline reaction time and to observe for directional change following repetitive thumb movements in different direction according to their initial TMS-evoked default angle. We introduced a manipulation of target uncertainty vs. frequency to systematically dissociate between the directional biases. After a TMS and goal-directed

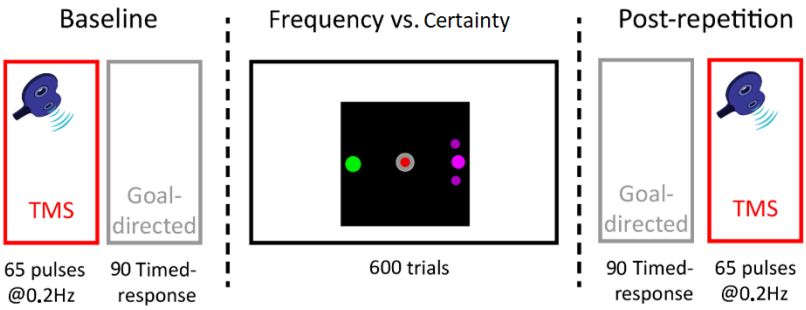

Figure 1. **Experimental Protocol**. After the baseline session, participants will perform 600 goal-directed thumb movements to one of four targets (315°, 330°, 345° and 210°).

baseline session, participants performed 600 goal-directed thumb movements to one of four targets (315°, 330°, 345° and 210°) (Fig. 1). The potential locations of the target on any given trial will not be equally probable; the repeated target at 330° will be presented in 30% of trials, whereas the two flanker targets at 315° and 345° will each be presented in 20% of trials. The distal target at 210° will appear in 30% of trials. By doing so, we divide the target space into two regions: (1) a more frequent region (centered on 330°) with greater uncertainty (increased variance), and (2) a less frequent region (i.e., 210°) with lesser uncertainty. Immediately after completing this training session, participants performed the post-repetition TMS session.

Results: Our preliminary results indicate that movement-bias is influenced by the frequency of previous movements rather than the certainty of upcoming movements. Unfortunately, at this stage, the result of the TMS-bias was not inclusive. We observed increased variability across participants in their TMS responses and it was difficult to conclude whether TMS-bias is more sensitive to frequency versus certainty.

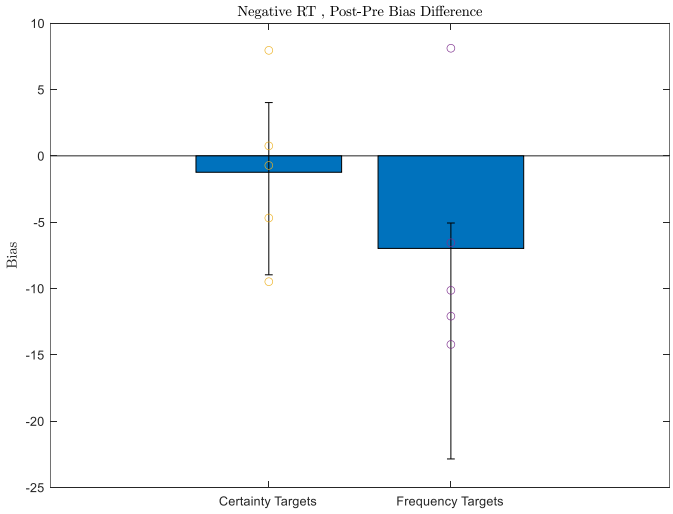

Figure 2. Bias difference between the mean bias post repetitive task and the baseline among all participants for certainty and frequency targets. Negative reaction time (RT) implicates only fast reactions (i.e., below average RT) were

Discussion: So far, our data suggests that TMS-biases and movement-biases co-exist and represent distinct processes of UDP. It seems that Movement-biases depend on movement-frequency, whereas TMS-biases are elusive. We believe that the small sample size is a limitation of the current conclusion, and more data is needed to significantly determine this.

Keywords: transcranial magnetic stimulation, use-dependent plasticity, neuroplasticity, motor cortex.

(22)

Bioreactor Design for Selective Differentiation of Stem Cells to Engineer a Thick, 3D Muscle and Adipose Tissue

Oryan Karni[1], Francesca Jaffe [1], Yedidya Zagury [1], Arbel Artzy-Schnirman[1], Shulamit Levenberg[1]

[1] Biomedical Engineering Faculty, Technion - IIT, Haifa, Israel

Introduction: Cultured meat is a new approach for producing meat *in-vitro* using tissue engineering techniques. The motivation is to revolutionize the food industry by solving pressing issues like reducing greenhouse gas emissions, global hunger, animal cruelty and health risks. One of the major challenges in creating cultured meat and in tissue engineering in general is creating a thick functional tissue composed of multiple types of cells. The challenges stem from diffusion limitations and maintaining multiple differentiation of co-culture simultaneously. While conventional meat contains muscle, fat and connective tissue, recent studies show the possibility of creating cell-based meat from muscle cells alone. In our study we attempt to create a thick tissue containing mesenchymal and satellite stem cells that differentiate simultaneously to adipocytes and muscle cells, respectively, in a bioreactor.

Methods: Using 3D printing techniques, a mold was designed and printed using a water-soluble filament (BVOH) and then fabricated with polydimethylsiloxane (PDMS) polymer. Punctured pipes were inserted to deliver the medium to the cells considering the diffusion limits, which were tested using live-dead assay. Mesenchymal stem cells (MSCs) were encapsulated in alginate inside the bioreactor and endured differentiation and maturation periods. Additionally, muscle differentiation was examined using C2C12 cell line that was encapsulated in alginate and endured a similar differentiation period. Afterwards, a dual bioreactor was designed to supply two different media to a specific area of the tissue. This was tested using MSCs with one-sided differentiation. The differentiation and maturation of all cell types were evaluated using immunofluorescence staining.

Results: Using a viability test, cell survival was observed when seeded in a bioreactor with punctured pipes vs. unpunctured pipes, which confirmed our model is effective. Adipogenic differentiation was observed throughout all areas of the tissue after differentiation and maturation periods. Muscle differentiation was observed only in specific areas of the tissue, possibly as a result of the lack of mechanical strength in the scaffold. The dual bioreactor shows partial success in differentiating area-specific tissue, further tests are needed to improve the findings.

Conclusions: There is a crucial need to deliver medium to cells within a thick tissue. The dual bioreactor could be the solution seeing that it shows the potential of inducing compartmentalized differentiation of a co-culture. In the future, this model can create a mature thick multi-cell tissue

designated to produce cultured meat. Another future use for this technique could be designing tissues, or even entire organs, for transplantation.

Keywords: Cultured meat, tissue engineering, bioreactor, diffusion.

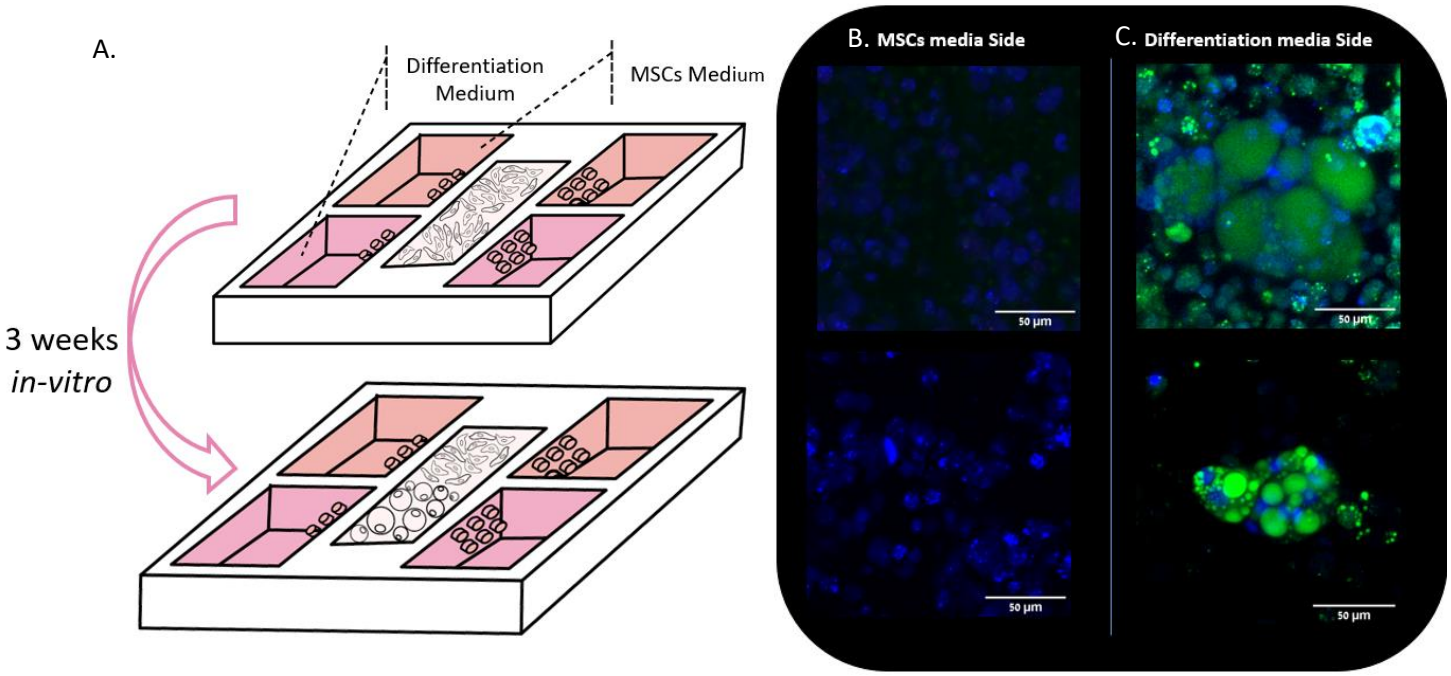

Figure 4- Model of MSCs in dual bioreactor. (A) Dual bioreactor illustration, (B) cells with MSCs medium, (C) cells with differentiation medium. Green; lipids, blue; nuclei.

(23)

Design, Development and Testing of a New Polymeric Heart Valve

Gal Pereg[1], Yevgeniy Kreinin[1], Oscar Lichtenstein[1], Netanel Korin[1]

[1]Faculty of Biomedical Engineering, Technion - IIT, Haifa, Israel

Introduction: The human heart has four valves, which can be damaged due to infectious disease, aging, heart attack and more. If that condition is left untreated, this can lead to heart failure and death. Today the common solution is doing a heart valve replacement. The implanted valve can be a biological tissue or a mechanical one.

Although the biological valve has a good and natural hemodynamic, since the valve does not get blood supply, it is not durable and loses its features after approximately 5-10 years. On the other hand, mechanical valves are durable but are very thrombogenic. Due to that, the mechanical valve requires the patient to consume anticoagulant drugs, which greatly endanger the patient's life and finally, after about 20 years, deteriorates too. Therefore, both types of valves do not make a definitive cure for heart valve replacements.

On this project, we developed a new kind of heart valve prosthesis, a polymeric one. We believe that the polymeric valve has the potential to be the future of heart valve prosthesis. It is made of durable, flexible material, and with the right design, can have a lower thrombus formation potential.

Methods: We have created the polymeric valve using 3D printing. The model of the valve is based on a biological native human valve. Since we wanted our final product to be made from silicone, we have printed the valve mold and not the valve itself. Then we have filled the mold with PDMS. After the mold becomes consolidated, we put it into an acetone bath. The resin (the plastic with which we have printed) dissolved and remained the silicone part alone. After creating the valve, we examined its functionality. We inserted the valve into an aorta model. Then we have connected the aorta model with the valve into the pulsatile flow system. The system is built from a pulsatile pump, a charging reservoir and two reservoirs with balloons, to resemble the ventricle and atrium mechanics. To examine the valve's thrombogenicity, we will conduct an experiment in which we inject Fibrin and Thrombin into the fluid. After the experiment, we will be able to count the amount of the clots accumulations.

Results: After several tries with different models and techniques, we have managed to receive a suitable, smooth polymeric heart valve prosthesis just as planned. When inserted into the pulsatile flow system, the valve has opened and closed according to the pressure gradient.

Conclusions: The durability and elasticity of polymeric heart valves are the features that turn polymeric heart valve prostheses into the bright future of prosthetic heart valves. In our work, we have successfully created a polymeric heart valve that is made from silicone. We have tested the valve to check its functionality and saw that the valve indeed open and close according to the pressure gradient created from the pulsatile pump.

Keywords: Heart valve; Polymeric; Thrombosis.

Figure 1: The prosthetic heart valve we have created.

(24)

Development of a Spheroid Model that Simulates Drug Penetration in Solid Tumors

Or Levy[1], Orel Shahadi[1], Maytal Avrashami[1], Hagit Sason-Bauer[1], Arbel Artzy-Schnirman[1], Yosi Shamay[1]

[1]Faculty of Biomedical Engineering, Technion - IIT, Haifa, Israel

Introduction: When investigating a drug or therapy intended for cancer solid tumors, two kinds of models are considered: two-dimensional (2D) and three-dimensional (3D). The 2D models set many problems since they fail to consider many crucial aspects of physiological conditions such as: extra-cellular environment, adhesion proteins, 3D micro-epoxy conditions etc. The existing 3D models present difficulties in monitoring drug penetration and in-tumor drug impact. The 3D spheroid model as presented in this research, consists of liver cancer cells extracted from mice that form the outer spheroid structure and green fluorescent protein (GFP) expressing fibroblast cells in its core. This model answers the problems familiar from other 3D models in general and spheroids models in particular; Its three-dimensional structure provides a good simulation of an in-vivo solid tumor and by monitoring the mean fluorescence intensity (MFI) given by GFP expressed in fibroblast cells core, we were able to evaluate the penetration of the drug inside the spheroid. In this research, we found an ideal formulation for creating reproducible spheroids, by choosing ideal concentrations of the two cell lines. The given model is tested with both free-drugs and drug carrying nano-particles produced in the lab.

Methods: The main players in the research are spheroids and drug carrier nano-particles. The spheroid is a combination of liver cancer cell line (SB2) with GFP expressing fibroblast cell line (3T3). The two cells populations are seeded together in an ultra-low attachment, round bottom plate which enables, due to lack of adhesion, the formation of a single spheroid in each well. The plate is incubated for 3 days to enable the formation of the spheroid, as observed under a "Lionheart" optic microscope.
The nano-particles are formed using a nano-precipitation method. These are dye-stabilized nanoparticles composed of a new dye that was developed in the lab (595) and Osimertinib, which is an anti-cancerous drug. The particles are characterized by Dynamic Light Scattering (DLS) to ensure gaussian distribution of size and by High Performance Liquid Chromatography (HPLC) to identify the free drug concentration in the nano-particles.

Results: We were able to quantify the ideal cell concentrations to develop a suitable uniform spheroidal model that includes constant spheroid size (diameter range of 300-400 μm), without

the formation of secondary spheroids (one spheroid per well) and with visible homogenous fluorescence in the core of the spheroid (average core diameter of $144.37 \pm 17.45\ \mu m$).

Osimertinib cytotoxic effect on fibroblast cells has been tested in 2D fibroblast cell cultures and in the spheroid model, demonstrating its efficacy as proven by monitoring mean fluorescent intensity (MFI) values. There is a GFP fluorescence descent as a function of drug concentration and time. This proves the correctness of the 3D model as the drug diffuses to the spheroid core and eliminates the fibroblast cells.

Conclusions: The 3D spheroid model meets the requirements, and hopefully in the future will provide a reliable basis for further research into the treatment of cancer.

Keywords: spheroid; nano-particles; three-dimensional; solid tumors.

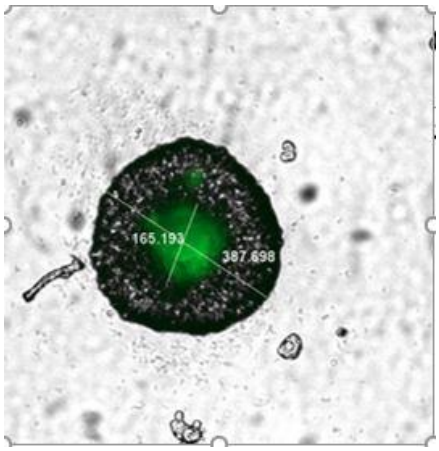

Figure 1: The modelled spheroid, with outer spheroid diameter of 387.698 μm, and inner fibroblasts diameter of 165.193 μm

(25)

Brain tumors segmentation from MRI data with deep-learning

Elinoy Faibish[1], Matan Kachel [1], Moti Freiman[1]

[1] Faculty of Biomedical Engineering, Technion - IIT, Haifa, Israel

Introduction: The most common type of primary brain tumors are gliomas, which arise from brain glial cells. Gliomas can be of low-grade (LGG) and high-grade (HGG) subtypes. High grade gliomas are an aggressive type of malignant brain tumor that grows rapidly and usually requires surgery and radiotherapy. Magnetic Resonance Imaging (MRI) is used extensively in diagnosis and treatment of glioma patients. An assessment of tumor volume and the exact structure and location is used for monitoring and surgery planning. However, as of today, these tasks are performed manually, require anatomical knowledge, are expensive, time consuming and can be inaccurate due to human error. Replacing the current procedure with automated segmentation and analysis would be of enormous value for improving diagnosis and treatment.

Methods: We implemented a deep learning model to preform semantic segmentation given MRI images. We explored different and advanced data augmentation to improve on the existing state-of-the-art models' performance.

We based our deep learning network on the well-established U-net model. In order to compere different data augmentation techniques, we introduced different changes (e.g., less convolution layers, less filters, etc.) to the model in an effort to shorten the training run time and achieve good results in less epochs.

In this context we explored two different models' architecture: 1) encoding the ground truth in 4 channels (3 labels + label for the background) and using Softmax activation for the network output, and 2) encoding the ground truth in 3 channels (with no label for the background) and using Sigmoid activation.

Lastly, we implemented a search function to search different augmentation policies in an automated way. Our search function was based on the Fast AutoAgument approach in which we refer to the augmented data as missing data points of training data.

Results:

The Sigmoid model achieved a superior performance.

	WT (Whole tumor)	TC (Tumor core)	ET (Enhancing tumor)
Sigmoid model	0.89	0.76	0.76
Softmax model	0.63	0.53	0.5

Conclusions: Data augmentation has huge potential for improving deep learning model generalization ability, especially for domains in which training data is scarce (e.g., medical images).

However, the large number of different augmentation policies and the hyperparameter tuning needed, requires development of an automated approach for searching appropriate augmentation policies for each dataset.

Keywords: Gliomas, Deep learning, Data augmentation, U-net

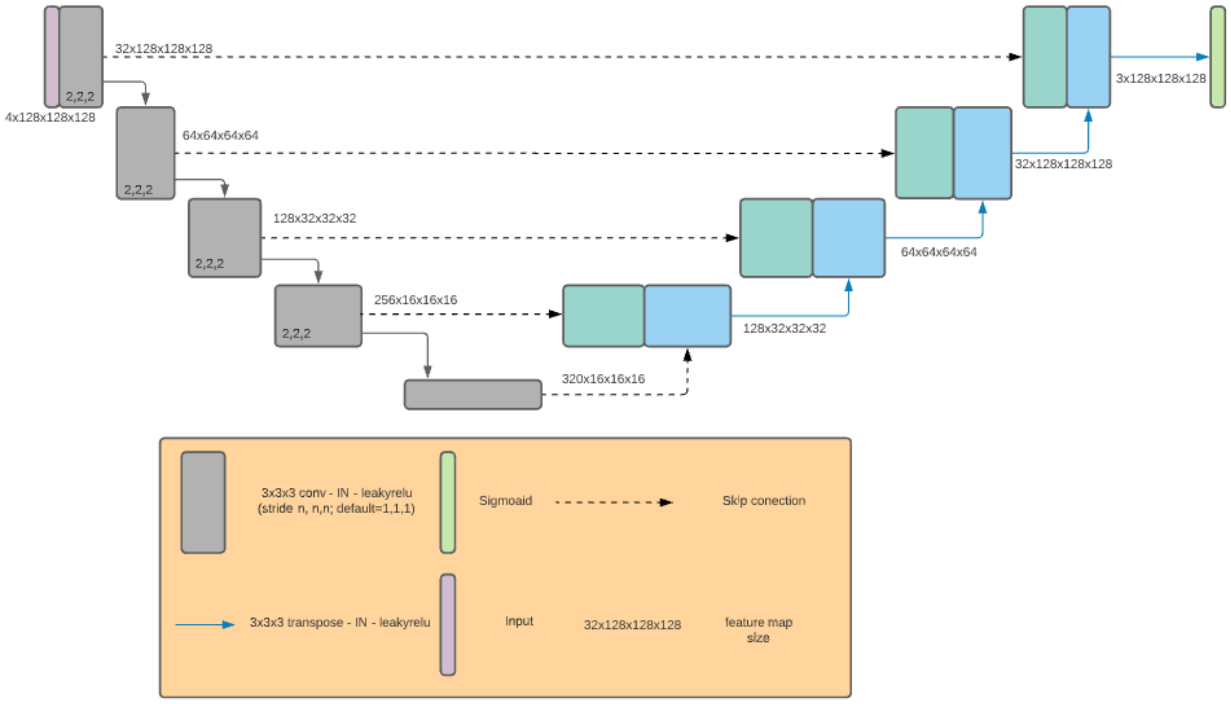

(26)

INFANT HEARING TEST USING EYE TRACKING

Suzan Shehady [1], Nardeen Badarny[1], Dr. Rola Farah[2] and Dr. Michal Zivan[2]

[1] Faculty of Biomedical Engineering, Technion
[2] Faculty of Education in Science and Technology, Technion

Introduction: Globally, over 665,000 infants are born every year with significant hearing loss. Early detection of infant hearing loss is critical to prevent delays in the infant's development of language, speech, and cognitive behavior.
The Current behavioral infant hearing test, Visual Reinforcement Audiometry (VRA) is a conditioning procedure, in which the child receives a visual reward (such as a mechanical toy) when he turns his head towards the auditory stimulus direction.
Limitations of VRA: infants are challenging subjects, their reaction is not always the defined head-turn an older child would present. Instead, slight body shivers or eye movement or even eye widening might indicate hearing the signal. In addition, it is a time-consuming procedure, that makes it difficult to maintain the infant's attention. Finally, VRA test requires a highly skilled audiologist in the testing room to maintain the child's attention, however, this audiologist might become a distractor as a foreign adult.

Aim: The current project is designed to build and test a prototype to determine whether behavioral hearing test (VRA) with eye tracking is a useful method as an objective, accurate and valid hearing test among children.

Methods: six adults (mean age 23- control group) and 19 children (age range: 1.8-2.7 years-mean age=2.4 years- experiment group) participated. Testing was performed in Sonic Center medical center in the audiology department and 4 frequencies were tested: 500, 1000, 2000, 4000 Hz in free field. A timeline was designed and set-up on Tobii pro Lab using X3-120 Tobii pro eye tracker. Tests were performed using real-time eye tracking, audiometer, with a conditioned video stimulus. Data was analyzed by a MATLAB code and compared to VRA/otoacoustic emissions results.

Results: Out of 19, 15 children passed the test with high gaze-data samples (more than 60%), while the other 4 children had a high percentage of data loss.
Data from adults demonstrated accurate eye movement but less interest in the visual reward.
Children, compared to adults, showed high interest in the conditioning procedure, and more seeking for the audio source. (Figure 5 and Figure 6).

More importantly, 5 out of 15 children did not turn their head during the VRA test, but they passed our eye-tracking test, as they only moved their gaze toward the auditory source.

Conclusions: Evaluations of the prototype show that VRA with eye tracking technology has prospects of success. Future innovations and projects implementing gaze contingency, synching audio source with a larger eye tracker will enable capturing more gaze data, automating the process, and testing a wider range of ages including challenging populations.

Keywords: gaze data, eye tracking, audiometer

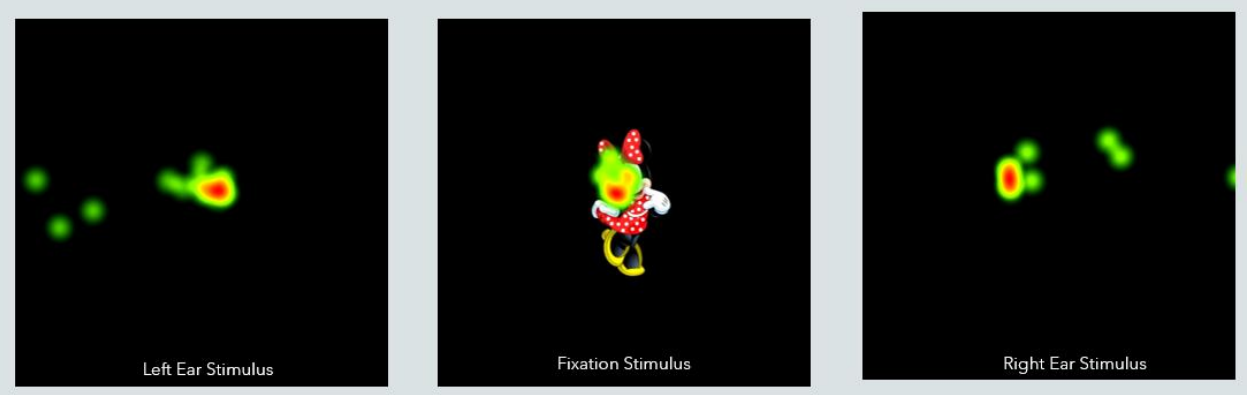

Figure 5 - Averaged Heat Map - control group (A – left ear, B – Fixation, C – Right ear)

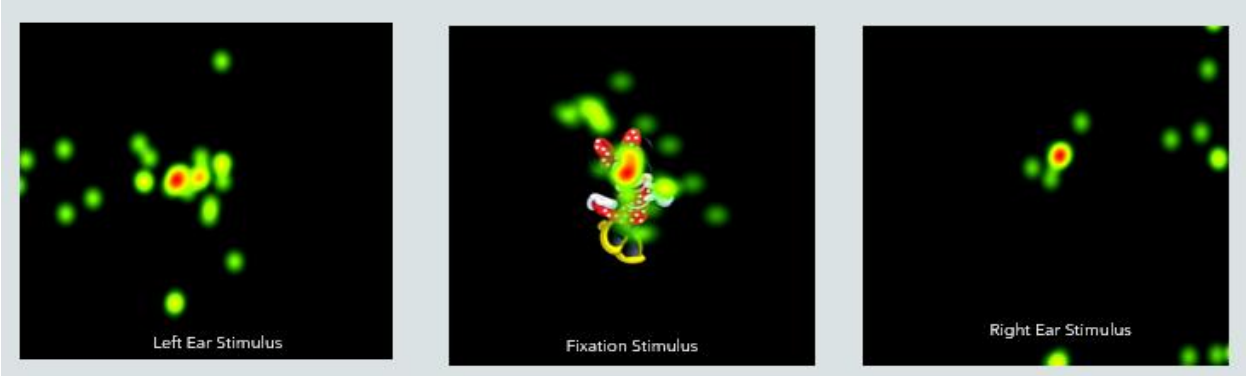

Figure 6 - Averaged Heat Map - children group (A – left ear, B – Fixation, C – Right ear)

(27)

Automatic Detection of LUS Characteristics and Specifically COVID-19 Related LUS Artifacts

Dekel Brav[1], Ehud Tal[1], Noy Mark[1], Lior Lupu[2], Dan Adam[1]

[1]Faculty of Biomedical Engineering, Technion - IIT, Haifa, Israel
[2]Department of Cardiology, Tel Aviv Sourasky Medical Center

Introduction: The Coronavirus disease 2019 (COVID-19), is a contagious disease causing severe acute respiratory syndrome coronavirus 2. The virus has spread worldwide, leading to an ongoing pandemic with 170,360,315 confirmed cases and over 3.5 million deaths around the globe. Computed tomography (CT) is the routine imaging technique for diagnosis and monitoring. Despite the high sensitivity, CT has several problems: it is not universally available, requires movement of an infected patient with potential exposure, etc. Recent studies suggest using lung ultrasound (LUS) as a solution, however no automatic classification system yet exists. To that purpose an automatic artifact detection model is necessary.

Methods: In order to detect the region of interest (ROI), which is the pleural line, sub-pleural area (areas greatly affected by the severity of the disease) and ribs, we approached designing a model based on a variety of image processing techniques: We used morphological methods such as gradient filters, feature detection algorithms such as SIFT, different types of transforms such as polar-cartesian transform, Radon transform, thresholding, and other algorithms.

Results: We implemented an analysis using 4 types of evaluation metrics: mean pixel accuracy, IoU, Dice coefficient and the Hausdorff distance metric. We will use the evaluation metrics mentioned above to evaluate the results as soon as we receive the ground truth data from the Ichilov cardiological center. For now, we manually checked 914 LUS scans with 813 of them segmented properly (88.9% accuracy) using a True/False metric. The feature detection algorithms and the Radon transform did not bear fruit, although some of their principles were integrated into our algorithm.

Conclusions: Detection of the ROI is achievable; we believe we have reached the necessary results to start the next step of the system – designing a neural network that will be able to take these segmented ROI as inputs in order to classify various aspects of LUS. For future work, when a significant dataset of segmented LUS scans will become available, we believe we could improve our results by using deep learning networks such as U-net or DeepLab to achieve higher results.

Keywords: COVID-19, image processing, pleural line, artifacts, lung ultrasound, segmentation

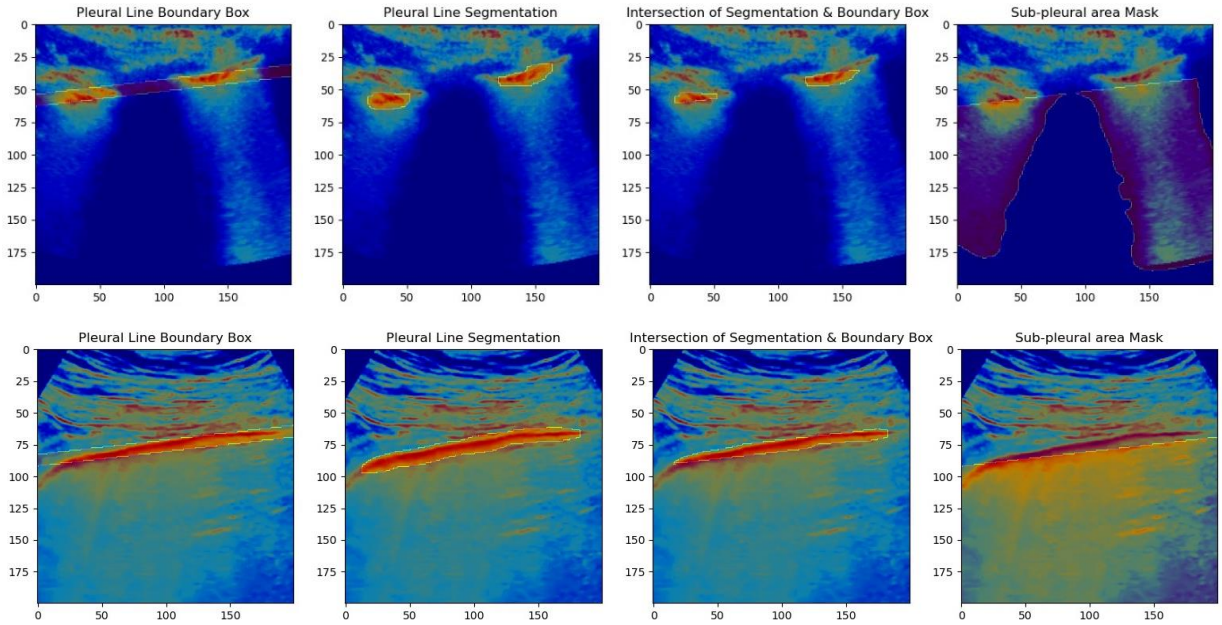

Figure 1: Detection of pleural line, ribs, and sub-pleural area

(28)

Red Blood Cell Based Drug Carriers for Targeted Delivery to Stenotic Arteries - an in Vitro Study

Shay Ohana[1], Ofir Kalman[1], Danielle Nemcovsky-Amar[1], Maria Khoury[1], Oscar Lichtenstein[1], Netanel Korin[1]

[1]Faculty of Biomedical Engineering, Technion - IIT, Haifa, Israel

Introduction: Cardiovascular diseases (CVDs) are considered one of the leading causes of death worldwide, accounting 31% of death cases in the world in 2016. CVDs include heart attacks, strokes, and pulmonary embolism, and are usually characterized by blockage of blood flow, which can lead to fatal consequences. Under pathological conditions, such as: vasospasm, narrowing of arteries (stenosis) occurs which is also associated with pathological level of high shear stress. These elevated levels of shear have been recently utilized for localized drug delivery to stenotic arteries and thus may lead to improved treatments. In this study we will examine the use of red blood cells (RBCs), as drug carriers, for targeted drug delivery to stenotic arteries. Our hypothesis is that in stenotic regions, where RBCs drug carriers are exposed to high shear stress, agents will be released more effectively.

Methods: Real-sized models of stenotic human arteries (4 mm in diameter) were 3D printed and fabricated from polydimethylsiloxane (PDMS)/Elastosil silicone with different percentages of stenosis: 0%, 75% and 90%.
Fluorescently Tagged-Dextran of several molecular weights 20, 40 and 70kDa, were encapsulated into RBCs using the hypotonic dialysis method. After the encapsulation process, the RBCs were diluted with phosphate buffered saline (PBS) (-,-) and circulated in a closed-loop perfusion system using a peristaltic pump (Watson Marlow 530C, Watson) for 1 h at a flow rate of 200 ml per minute through the models.
Qualitative and quantitative examinations of the RBCs' fluorescent degree, before and after performing the encapsulation and after the perfusion experiment, were performed using confocal microscope and Fluorescence Activated Cell Sorting (FACS) respectively.

Results: After the encapsulation process, RBCs showed high fluorescent values in both qualitative and quantitative examinations relative to washed RBCs (non-capsulated), which indicates successful encapsulation. Moreover, small molecular weights (20 and 40 kDa) presented higher fluorescent values. Our results reveal that dextran was released from the RBCs in stenotic models (75% stenosis) 2 times more than straight models (with 0% stenosis), which confirms that higher values of wall shear stress (WSS) have an impact on the release process.

Moreover, a higher degree of release was observed under 90% stenosis compared to 75%, supporting that release may be shear dependent.

Conclusions: Leveraging the high shear at stenotic arteries, RBCs drug carriers can be designed to allow localized drug delivery at these sites. Moreover, the more drastic the stenosis is, the higher the rate of release of the encapsulated agent from the RBCs carriers.
This platform may be used for exploring the targeting of different therapeutic agents to stenotic arteries, which may lead to more effective treatments.

Keywords: Red blood cells, Drug Delivery, Hypotonic Dialysis, Shear stress, Stenosis

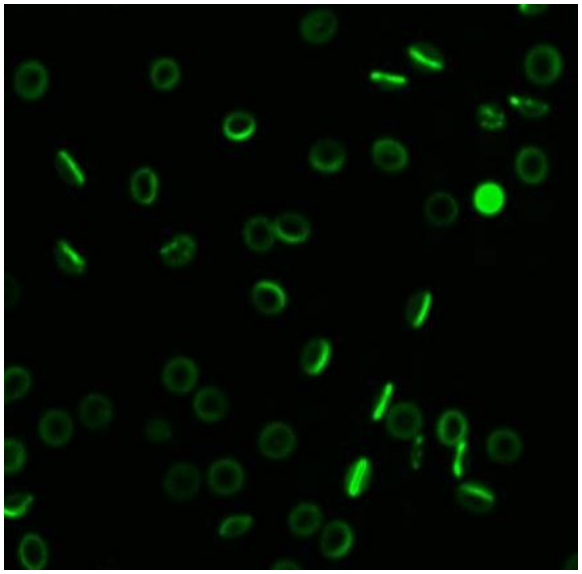

Figure 1: Confocal image of RBCs loaded with fluorescently tagged-Dextran (40kDa) following a perfusion experiment through a stenotic model (90% stenosis). Scale bar: 10 um.

(29)

Suppressing the Reflex Response by Exposure to Weak Pre-Pulse in the Startle Circuit of the Larval Zebrafish

Asaf Tzur, Yakir Yemini, Dor Meron, Michal Zivan, Limor Freifeld

Faculty of Biomedical Engineering, Technion - IIT, Haifa, Israel

Introduction:

To maintain normal brain function, information is filtered such that the irrelevant data is decreased. A major example of this mechanism is the PrePulse inhibition, known as PPI – diminishing the startle circuit's response using a preceding stimulus. Damaged PPI mechanism is linked to several neurological disorders such as schizophrenia. To ease this mechanism's learning process, one can use the simpler model of Zebrafish; these have a rather facile nerve system. Examining the results of the PPI mechanism may assist us in discovering new information about the neurological paths of the human nerve system.

Methods:

To begin with, a model of first quantification was built to find out the weak pulse' intensity. A petri dish containing Zebrafish was placed under a macroscope along with an actuator which creates the stimuli. The actuator's movement was controlled by a computer software. 6 different intensities were tested. To differ between those intensities, we altered the time interval between the actuator's drop to its rise. After determining the weak pulse, we changed the software's code to create our two scenarios: regular pulse only and a weak pulse followed by a regular one. 20 iterations of each scenario were conducted per experiment such that each one included a total of 40 random iterations. The randomization took place to refute any chance of adapting to the stimuli, and 3 time intervals were tested between the two pulses: 300,400 and 500 milliseconds. Since a tap stimulus is considered normal if approximately 80% of the fish responded, experiments that exhibited less than 60% response were excluded.

Results:

To determine whether the regular pulse matches our hypothesis, we used the data from all the experiments. The total amount of examined fish is 414 from which 320 responded. Thus, we do not reject the null hypothesis which is that our stimulus is considered regular with 8.4% level of significance (P-value is 0.084).

In the 500 interval, 180/234 (76.9%) responded to regular stimulus whereas 90/268 (33.6%) responded to the PPI scenario. The confidence interval with 99% level of reliability to the proportion's difference is [0.33,0.54].

In the 300 interval, 93/120 (77.5%) responded to regular stimulus whereas 29/114 (25.4%) responded to the PPI scenario. The 99% confidence interval is [0.38,0.66].

Conclusions:

Looking at the above confidence intervals, we can see that 0 is not there. Thus, we infer with 99% confidence level that there is a reduction between the two proportions.

We chose 500 as the optimal time interval. Although the results were slightly better for the 300 interval, we based our choice on a published article rather than on only 2 experiments. According to the confidence interval, the reduction's value goes between 33% - 54%.

Keywords:

PPI, Larval Zebrafish, C-bend, Startle circuit.

Figure 1: The typical C-Bend caused by an external stimulus under our macroscope.

(30)

The Opposing Effects of Hematopoietic Glucose Uptake for Leukocyte Production in Diabetes and G-CSF Treatment by Retrospective ^{18}F-FDG PET/CT Analysis

Bashar Shehadeh[1], Adi Daoud[1], Katrien Vandoorne[1], Michal Weiler-Sagie[2]

[1]Faculty of Biomedical Engineering, Technion - IIT

[2]Nuclear Medicine Department, Rambam Health Care Campus, Haifa, Israel

Introduction: Leukocytes, also called white blood cells, are descendants of hematopoietic stem and progenitor cells and are made in the bone marrow. In the past few years, researchers began to understand that type 2 diabetes is not merely a metabolic disorder; it is a disorder where inflammatory responses are altered, leading to increased cardiovascular risk in type 2 diabetes. However, it remains unclear whether elevated white blood cell count, a phenomenon present in type 2 diabetes, is accompanied by enhanced proliferation of hematopoietic stem and progenitor cells with subsequent increased glucose uptake. On noninvasive ^{18}F-FDG PET/CT, glucose uptake can be measured. In this study, we aimed to assess the glucose uptake in hematopoietic organs (spleen and bone marrow) in patients with enhanced white blood cell counts, namely in diabetic patients and non-diabetic patients after G-CSF treatment.

Methods: In this retrospective study, 60 oncology patients without bone marrow lesions that underwent ^{18}F-FDG PET/CT scan were enrolled: non-diabetic controls, type 2 diabetes patients, and non-diabetic patients after G-CSF treatment (20 per group). Standardized uptake values (SUVs) were measured on whole-body ^{18}F-FDG PET/CT scan by selecting volumes of interest (VOI) for several organs: spleen, bone marrow of lumbar vertebra 4 (L4), and thoracic vertebra 7 (T7) bone marrow, liver, and the aorta (blood pool). L4 and T7 SUVs were averaged to represent bone marrow uptake. Bone marrow and spleen uptakes were attuned for background uptake in the liver and in the aorta. Hematological parameters such as white blood cells count, red blood cells, and neutrophil count were also assessed.

Results: The SUVs, expressed as mean±sem, were significantly lower in diabetic patients compared to the non-diabetic controls: aorta-normalized SUVs were 1.008±0.0.0567 and 1.321±0.107 for bone marrow of L4/T7 non-diabetic control and diabetic patients respectively (P = 0.014). The spleen uptake was also decreased in diabetic patients. However, the G-CSF group

exhibited significantly higher SUVs in both the bone marrow and the spleen when compared to the both groups. Furthermore, white blood cell count was highest in the G-CSF group and lowest in the non-diabetic control group. No significant differences were observed in red blood cells count and neutrophils count between the diabetic group and the non-diabetic control group.

Conclusions: Type 2 diabetes is associated with higher WBC counts, yet lower glucose uptake at the bone marrow and the spleen, reflecting reduced glucose metabolism at these sites. Whereas G-CSF treatment led to higher WBC counts and higher ^{18}F-FDG uptake at the hematopoietic organs. In G-CSF, the enhanced glucose uptake can be explained by the enhanced hematopoietic stem and progenitor cells proliferation present after G-CSF treatment, with consequent enhanced WBC in the blood. It remains to be determined, how WBCs are produced excessively in diabetes without increased glucose uptake. This research initiates further questions on hyperglycemia aberrant cell proliferation at the hematopoietic organs and whether cell proliferation works with altered mechanisms that can be specifically targeted.

Keywords: PET/CT, 18-F-FDG, Diabetes, Inflammation

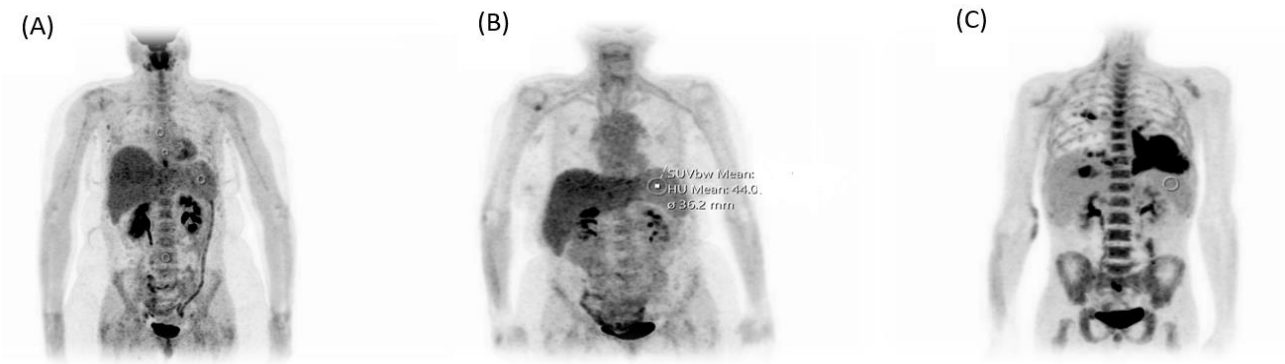

Figure 1: (A)Glucose uptake in hematopoietic organs in control non-diabetic patients was (B) decreased in diabetic patients and (C) substantially increased in patients after G-CSF treatment.

(31)

System development for ECG noise sources detection and classification in Electrophysiology labs during clinical operations of heart arrhythmia patients

Nitzan Gorani[1], Gaia Levin[1], Tsafrir Ozer[2], Firas Mawase[1]

[1]Faculty of Biomedical Engineering, Technion - IIT, Haifa, Israel
[2]Biosense Webster company part of J&J family, Yokneam, Israel

Introduction: Arrythmia is one of the major threats to human life. In 2018, arrythmias were the primary cause of death in 53,895 deaths. The most common is AF (Atrial fibrillation)- 0.51% of the worldwide population suffers from AF, while it is prevalence has increased by 33% in the last 20 years. The way to diagnose it, is by using an electrocardiogram (ECG) signal that possesses critical information about cardiac functionality. Carto is a system that treats arrhythmias in a minimal invasive manner. It can be used to map and navigate inside the heart and receive ECG signals from the patient during a procedure. While 52% of hospitals in the world use Carto system, customers have brought a number of complaints to light of which the second largest is noise ECG interference. The system has algorithms that reduce noises but the algorithms have difficulty in filtering specific noises to prevent the filtering of physiological signals. In this article, a solution has been proposed to deal with this problem- identifying noises and their sources and suggesting actions that can be taken to reduce them. This solution will improve the performance of the system and thus will allow for better and more accurate care that will save many people's lives. In addition, it will save time and money.

Methods: Using an algorithm (written in "Mathematica") based on an existing algorithm in Carto system that analyses ECG signals in the frequency domain. Cases were taken from database from several laboratories (n=7). The analyses were performed on signals from chosen channels which receive signals from different locations of the heart. The algorithm detected quiet areas (without pacing and ablation, $t = 50[sec]$) and analyzed rare physiological frequency range ($30 \leq f \leq 300[Hz]$). The algorithm searched the number of occurrences of each frequency and calculated its absolute and relative intensity. The output is a table that combines all of the frequencies identified as noise and their intensity values. In addition, an FFT graph of the signals of each channel is displayed. The source of the noise is identified by comparing the frequencies detected to known frequencies. Moreover, an experiment was performed in an EP lab in which known noises were inserted into the system and the data was analyzed.

Results: The laboratories tested were identified as expected as noisy or quiet. In the noisy labs, the algorithm detected a higher number of frequencies whose relative intensity exceeded the

defined threshold value ($Th = 5$). In addition, the noises which were detected were classified into two main categories: environmental and systematic. In the EP lab experiment, the algorithm detected frequencies which characterizes the noise sources according to expectations.

Conclusions: The algorithm enable to define whether the lab is noisy or quiet and to characterize the noise sources during a procedure. This characterization assists the clinical team in improving the procedure conditions and specify the actions that need to be taken in order to get a cleaner ECG signal. In the future, the algorithm will enter as a feature in the Carto system and run on all existing channels in real time procedures. In addition, the feature will work as a machine learning, it will add new identified frequencies and successful actions to the system database.

Keywords: Noise detection; Noise classification; ECG signals; Arrhythmia

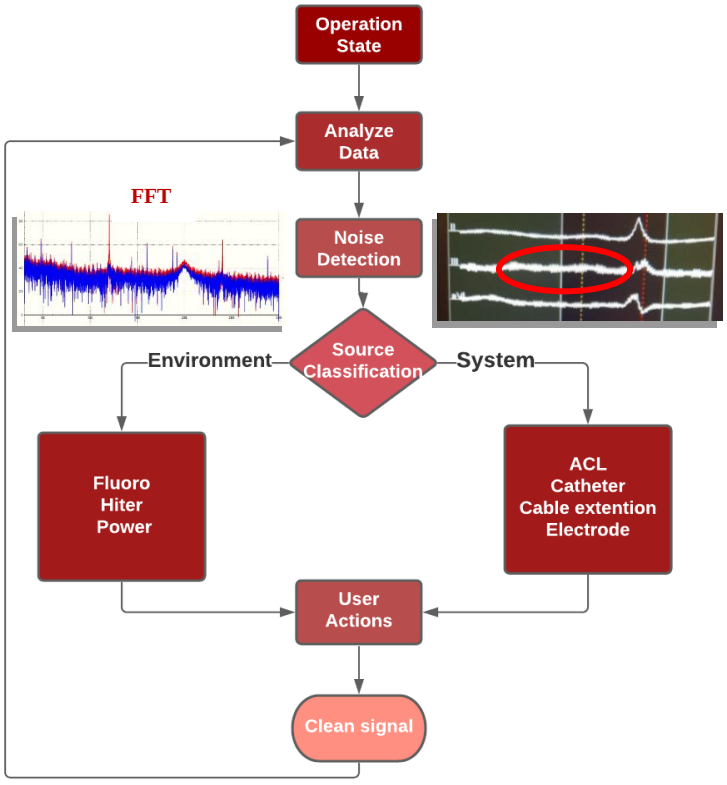

Figure 7: Identifying noises and their sources - solution flow chart

(32)

A Whole-Cell Bacterial Biosensor for L-lactate Detection in Urine

Rami Eid[1], Jawan Asla[1], Valeriia Kravchik[1], Ramez Daniel[1]

[1] Faculty of Biomedical Engineering, Technion - IIT, Haifa, Israel

Introduction: Lactic acid, a carboxylic acid molecule, it is produced by most tissues in the human body as the product of anaerobic metabolism. Lactate exists in two isomers (L-lactate and D-lactate). Current lactate measurements only include L-lactate which is the primary isomer produced in humans.
The concentration of lactate in the blood depends on the rate of production and the rate of liver clearance, so increasing urine lactate concentration indicates the increasing of blood lactate concentration. Measuring urine lactate concentrations can reveal information about patient's clinical state, and they can help us evaluate various pathological states and diagnose diseases.
Whole-cell bacterial biosensors consist of biological elements, typically genetically modified bacteria. Such bacterial cells include sensory components fused with fluorescent proteins. In this research we create an ultrasensitive whole-cell bacterial biosensor fermented by host cells, with high sensitivity and specificity to L-lactate in urine, and the data we got are integrated with signal processing tools.

Methods: We present an L-lactate biosensor based on genetically engineered Escherichia coli (E. coli); This system was constructed on two plasmids which can generate light energy (GFP) when it detects L-lactate molecule. These plasmids were constructed using basic molecular cloning techniques. And transformed into E.coli using a standard heat shock protocol.
The light energy signal is measured using plate reader. Culture aliquots were mixed with various concentrations of L-lactate (0-10 mM) and grown in Luria-Bertani (LB) Broth and added to the urine sample.
Furthermore, in the last step we built a theoretical model which supported by experimental results that excellently matched the measured bacterial light signal.

Results: The results shown in Figure 1a shows the GFP expression as a time dependence for 16 hours with synthetic urine and different concentrations of lactate, the GFP expression increase until reaching to a steady state after approximately 700 min.
The dose−response curves (Fig 1b) describe the system behavior as an input−output transfer function after reaching the steady state, in a way that the GFP expression at a specific time point is displayed as a function of lactate concentrations. In this graph we can see the GFP expression as a lactate dependence that taken from an actual experiment. In addition, we can see an optimization curve (fitting) extract from these results, this optimization curve shows the behavior

of the system as dependent on different lactate concentrations without noise caused by various system components and measurement errors.
Finally, in this graph we also show the behavior of the system with the addition of random noise, this noise can help us simulate the same experiment and build a machine learning system that will allow us to match different GFP expressions to different lactate concentrations.

Conclusions: In addition to the various lactate detection methods, whole cell biosensors with improved computing and amplification capacity could meet clinical requirements and should enable new approaches for medical diagnosis. In addition, our results indicate the way forward for future work, highlighting the improvements required for clinical-level accuracy, which could allow for detecting lactate in the urinary tract and help in early diagnosis of diseases.
Keywords: Biosensor, L-lactate, Urine, Synthetic biology.

a. b.

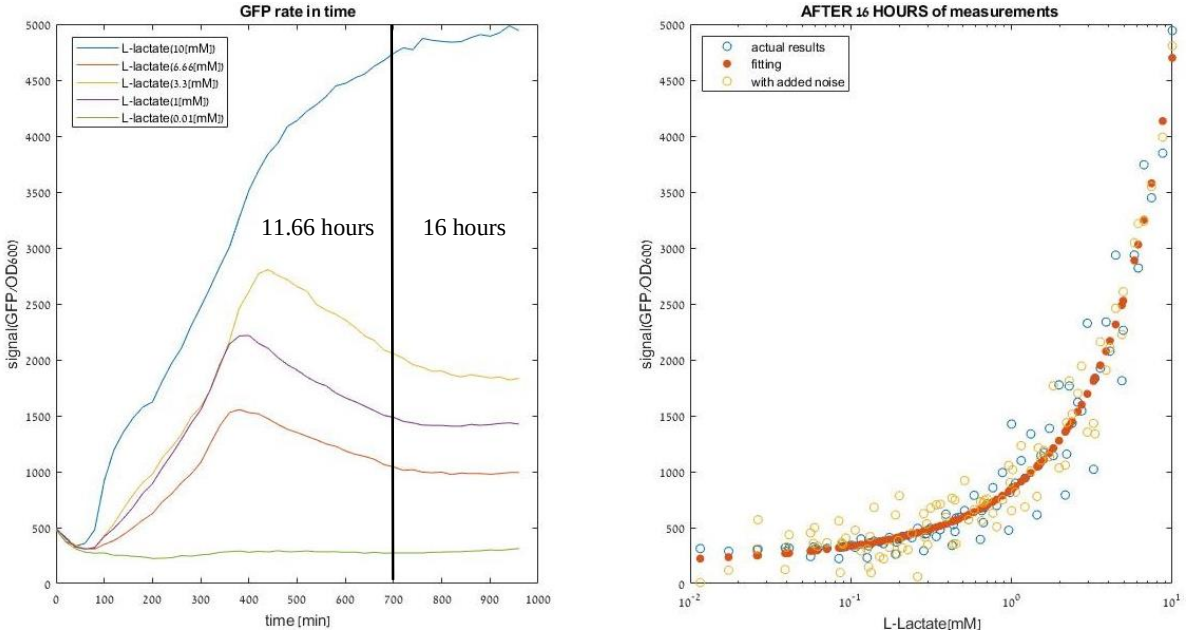

Figure 1: (a) GFP expression as a time dependence, (b) Dose−response curve with experment actual results, optimization curve and added noise after 16 hours of measrmunts

(33)

Evaluation of Mental States with a Mood Tracking Smartphone App

Daniel Sapir[1], Menucha Meir[1], Miri Cohen[2], Yossi Shamay[1]

[1] Biomedical Engineering Faculty, Technion - IIT, Haifa, Israel
[2] Faculty of Social Welfare and Health, University of Haifa, Israel

Introduction: Many human studies question the effect of mental state and mood in biomedical fields such as immunology and cancer immunotherapy. Today, psychological stressors are diagnosed through questionnaires or clinical interviews with professionals performed every 3-6 months. We hypothesize that these studies can benefit from continuous monitoring of patient's mood over time. There is still no accepted method to test this hypothesis. There are quite a few smartphone apps on the market today, which aim to track mood in various ways, including emojis based micro-journals. However, these apps are not adapted for clinical settings because they are not confidential or blinded, the data is not stored or curated for analysis, and there was never an attempt to evaluate their biomedical value in with statistical tools.

Methods: In our study, an in-house, user-friendly smartphone application was optimized and tested to perform daily monitoring of the subject's mood. Because it is not possible to use applications where the databases are visible to developers who do not take part in the study, a new application has been built in which the subject's information and the data they enter the in application will be kept confidential from foreign parties. An attempt was also made to create a simple, user-friendly application without the need of multiple readings or language comprehension.

In order to evaluate the application with the currently existing diagnostic methods, healthy participants with different demographic data were recruited for a two-week experiment. Participants were asked to fill out anxiety and depression questionnaires at the beginning and end of the experiment, and throughout the two weeks, filled out emojis daily in the app that reflected their mood at the time. In addition, at the end of the experiment, participants were asked to fill out a user experience questionnaire.

The experiment was conducted twice, at different times of the year, with some participants taking part both times and some only on one of the experiment dates. At the end of the experiment, the data was analyzed using various statistical tools such as correlation, regression etc.

Results: Data of 85 healthy participants over a two-week period was acquired using the app (1790 data points). We show that there is a good correlation between the app and the mood questionnaires, especially between the second depression questioner. In addition, the app has a significant advantage for the needs of the research, as it attests to the mood of the participant in high resolution and day-to-day over a continuous period which is not feasible with a onetime questioner.

Conclusions: Mood recognition is a complex and dynamic process. We anticipate that the tool we have developed may help characterize a subject's mood over time. Further dynamic and ongoing diagnosis of depression or anxiety may be a tool for researching the relationship between the effect of mood on immunotherapy treatments, and on other studies dealing with the effect of mental states on various situations.

Keywords: App; Mental state; Statistics; Immunotherapy.

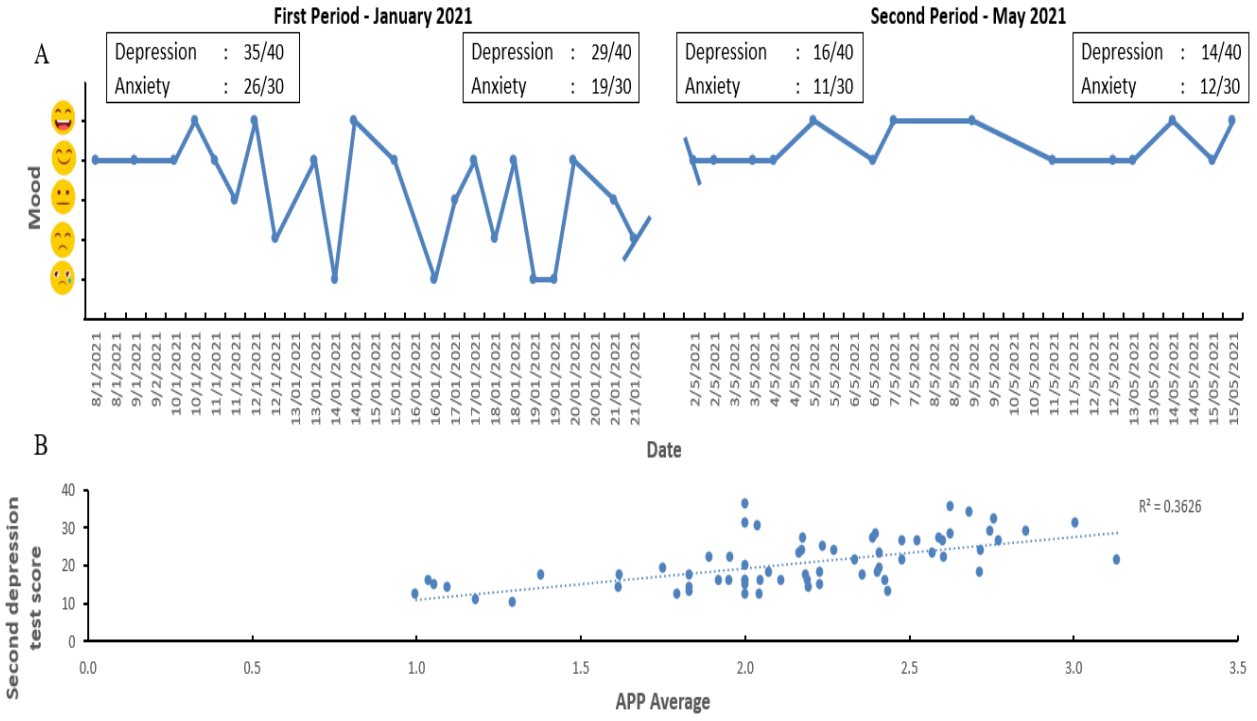

Figure 1. A) Records from the app and scores of depression and anxiety tests of a single participant during two different periods (January and May). B) Correlation between app average and second depression test score

(34)

Preparation of Nanoparticles for KRAS P53 Derived Lung Cancer

Liana Shalabi[1], Salma Khateeb[1], Yuval Harris [1], Arbel Artzy-schnirman[1], Yosi Shamay[1]

[1] Biomedical Engineering Faculty, Technion - IIT, Haifa, Israel

Introduction:

Lung cancer, also known as lung carcinoma, is a malignant lung tumor characterized by uncontrolled cell growth in lung tissues. This growth can spread beyond the lung by the process of metastasis into nearby tissue or other parts of the body. In this project, we research a NSCLC (Non-small cell lung carcinoma) KRAS P53 derived lung cancer. We highlight the problem that lays in the combination of both of KRAS P53 mutations, resulting in a "double proliferation signaling". NSCLC is usually treated by free drugs, which can be disruptive and toxic, furthermore it attacks and harms healthy tissues or cells. Using targeted nanoparticles which we have prepared, offers many advantages such as improving drug delivery and overcoming many problems associated with conventional drugs.

Methods:

According to our initial findings regarding free drugs, we have found that Trametinib offers the best results in forming Nanoparticles compared to the other drugs which were involved in our research. Thus, we have decided to try different combinations of Trametinib with other drugs and observe its effect on spheroids (a 3D model for cancerous tumor). We researched which drugs works best combined with Trametinib and found that Paclitaxel and Linsitinib may offer an effective combination with Trametinib. We did a 2D KPL cell culture experiment with these drugs combination (Trametinib+Paclitaxel, Trametinib+Linsitinib). Next step was preparing Nanoparticles from these drugs with IR-595 as a dye stabilizer in order to check which drug/drug combination works best as Nanoparticles.

After preparing these Nanoparticles, we did a 3D KPL experiment with free drugs and Nanoparticles, each on different plate (ultra-low attachment round bottom-ULA plate for 3D experiment, and flat plate for 2D, with same conditions for both) and then compared the two.

It is a known fact that KPL patients acquire a resistance to Trametinib. We wanted to check whether our combinations worked on cells created in the lab that acquired such resistance.

Results:

According to our results, we have found that Paclitaxel and Trametinib Nanoparticles combination is the best out of all in decreasing the spheroids size. Whilst, according to DLS results Linsitinib Nanoparticles were the least effective among all the others. We should note that Linsitinib as Nanoparticles as well as free drug, worked the least on the spheroids, but the combination of Linisitinib and Trametinib worked very well in doing so.

Conclusions:

In terms of NPs and FD, we conclude that NPs work best on KPL cancer cells. It is known that blood vessels that cancer tumor creates for itself is perforated, Thus Nanoparticles rely on that fact, which allows them to have easier accessibility to the tumor's location.

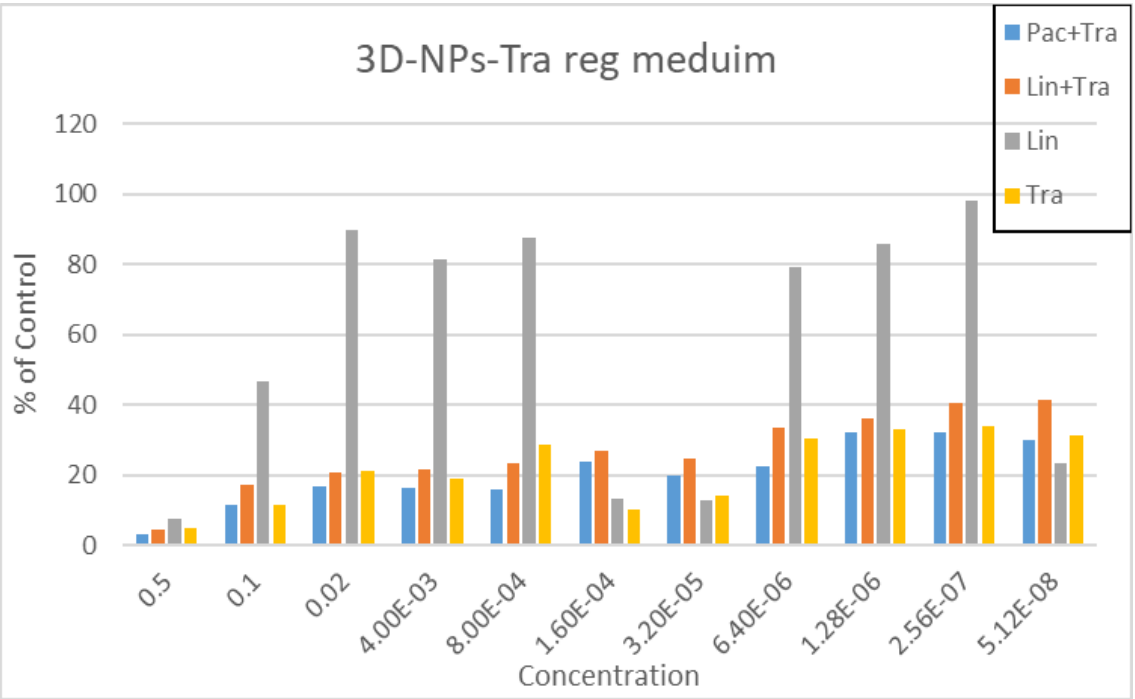

Figure 8: Nanoparticles effect on 3D cancer models.

(35)

Detecting Stenosis in the Carotid Arteries Based on SCG and Acoustic Signals.

Elias Bisharat[1], Noa Bachner-Hinenzon[2], Oscar Lichtenstein[1]

[1]Facult of Biomedical Engineering, Technion - IIT, Haifa, Israel
[2]Sanolla, Nesher

Introduction: Carotid Artery Disease (CAD) occurs when fatty plaques and deposits build up inside the carotid artery, resulting in stenosis or narrowing of the artery. The obstruction of blood flow to the brain can deprive the brain of oxygen and lead to stroke. Stroke is the one the most common causes of death and the leading cause of permanent disability. Moreover, rupture of the plaque can occur, and small pieces of this plaque can travel inside the brain and block other smaller arteries and deprive the afflicted location of oxygen which can lead to cell death. In addition, increases blood flow velocity can lead to aneurysm. The diagnosis of CAD is done after major symptoms using scanning tools that are only available in hospitals, increasing the risk for permanent damage. The need for noninvasive, fast, cheap and readily available method for the detection of carotid stenosis is required in order to achieve early diagnosis to prevent stroke.

Methods: We used Computational Fluid Dynamics (CFD) software – Ansys Fluent to simulate non-Newtonian blood flow through an occluded and regular carotid artery that was modeled using SolidWorks, with close to real-life parameters. We analyzed the blood flow characteristics using the software numerical solution methods by solving the Navier-Stokes equation and continuity equations, comparing wall static pressure, shear stress and blood flow velocity. We used Sanolla proprietary smart electronic stethoscope VoqX^{TM} to capture SCG and acoustic signal from healthy carotid arteries and occluded carotid arteries. VoqX^{TM} can detect and record infrasound and audible sound, and using frequency shifting algorithms, it converts the infrasound to audible sound. It can also display, record and send different sound signature images and data for analysis. Acoustic signals were analyzed via MATLAB software, using spectral analysis and algorithms.

Results: There was significant difference between the blood flow characteristics of the two carotid artery model, comparing static wall pressure, wall shear stress and blood flow velocity. The acoustic signals that were recorded showed specific differences between the acoustic signature image of the occluded and non-occluded artery. Further spectral analysis with signal envelopes also showed different features.

Conclusion: The CFD model showed specific differences in the blood flow model which predicted different SCG and acoustic signal features. Spectral analysis of the acoustic signals

from the arteries can be used to detect occlusion in the carotid artery. This analysis can be implemented into the stethoscope to show real-time results in doctor-patient visits.

Keywords: Carotid Artery Stenosis; Stroke; Computational Fluid Dynamics; Infrasound; SCG; Acoustic Signals

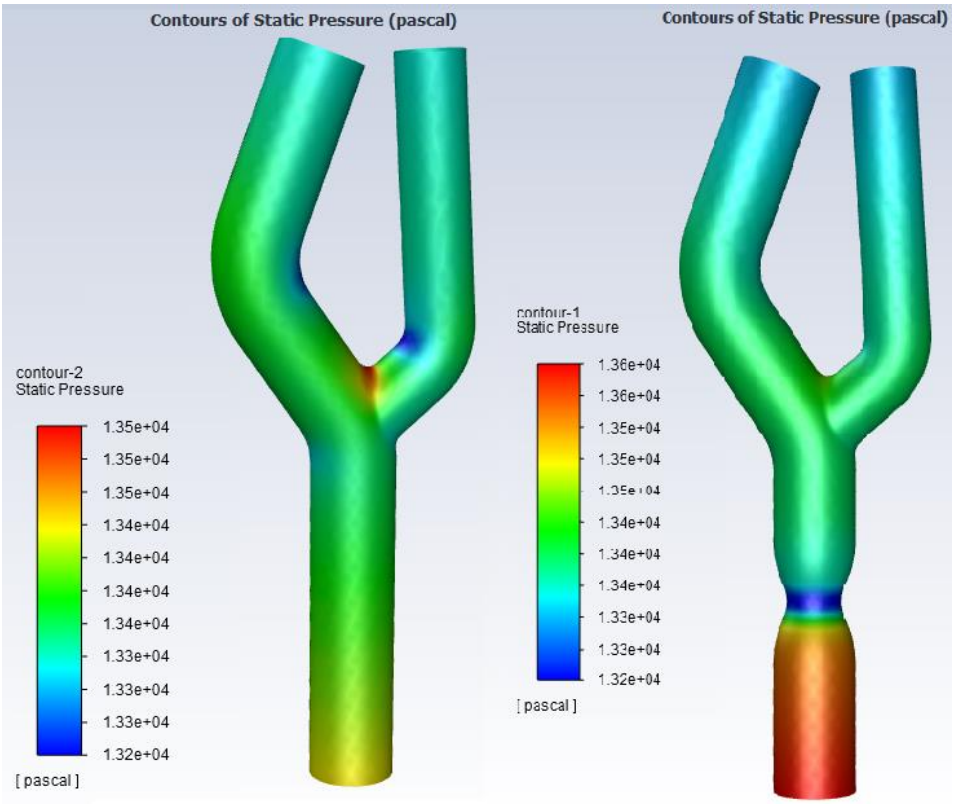

Figure 1 – Wall Static Pressure of the Carotid Artery during blood flow.

(36)

Semi-automatic Classification of the COVID-19 disease based on Lung Ultrasound

Mor Ventura[1], Omri Magen[1], Ehud Tal[1], Noy Mark[1], Lior Lupu[2], Dan Adam[1]

[1]Faculty of Biomedical Engineering, Technion - IIT, Haifa, Israel
[2]Department of Cardiology, Tel Aviv Sourasky Medical Center

Introduction: Coronavirus disease 2019 (COVID-19), is a contagious disease causing severe acute respiratory syndrome coronavirus 2. The virus has spread worldwide, leading to an ongoing pandemic. Computed tomography (CT) is the routine imaging technique for diagnosis and monitoring. Despite the high sensitivity, CT has several problems: availability, convenient accessibility to the patient, etc. Recent studies suggest using lung ultrasound (LUS) and COVID-19 severity grading systems as a solution, however no automatic classification system yet exists. Classification of the COVID-19 severity degree [0-3], in a fast and accurate way, has found to be highly essential and is expected be a great tool in reducing the workload on healthcare facilities. Additional parameters such as pleural line regularity or consolidation are found to be relevant for acquiring a full image of the patient's respiratory state.

Methods: In order to use deep learning methods, we needed a sufficiently large ground-truth (GT) database of labeled LUS videos of COVID-19-positive patients. Collaborating with Ichilov hospital's radiology department, we acquired hundreds of videos, that are currently in the labeling process. Using classic image processing and our own labeling (based on our training at Ichilov hospital), we created a temporary dataset which contains 794 segmented LUS scans that were used as input to our convolutional neural network (CNN). After examining different APIs, we decided to work with the open-source library *TensorFlow-Keras*. By reviewing different approaches in our research of the deep-learning field, we set the CNN architecture so it provides multiple outputs as following; it is built by sub-net branches, each classifies a different parameter and is weighted according to its relevance relative to the overall loss. For determining hyper-parameters, we used the K-fold method, and priors from similar multi-output nets which are trained on large scale datasets.

Results: On our temporary dataset, we have achieved 84.27% accuracy in grading the COVID-19 severity [0-3], 96.65% accuracy in classifying pleural line regularity, and 93.09% accuracy in classifying the appearance of consolidation. Due to the fact that our model is trained on data that is classified by us (not professional radiologists at Ichilov hospital), we believe that the network has a hard time extracting the right features in order to label the data correctly. The labeled data

is beginning to flow in rapidly and we are sure that when we use this data our results will drastically improve.

Conclusions: Classification of LUS can be a challenging problem, especially with an imbalanced dataset, but as we saw in the results above, we achieved a reasonably high score even with a limited dataset. For future work there are many ways to improve the network, such as further tuning hyper-parameters, testing different types of data-augmentation, using pre-trained networks, and much more.

Keywords: COVID-19, image-processing, deep-learning, classification

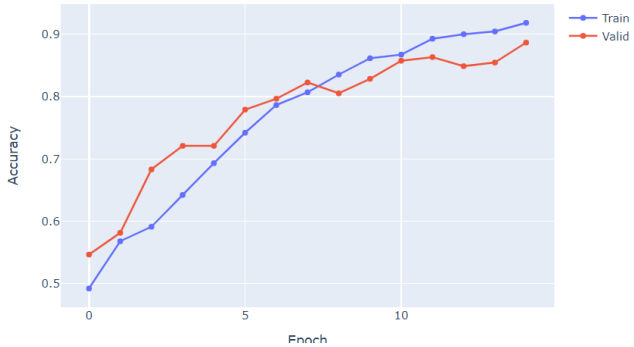

Figure 1.a: Accuracy vs. Epoch of COVID-19 severity grade

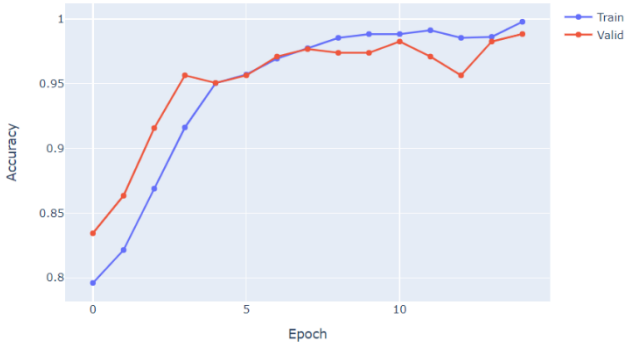

Figure 1.b: Accuracy vs. Epoch of pleural-line regularity

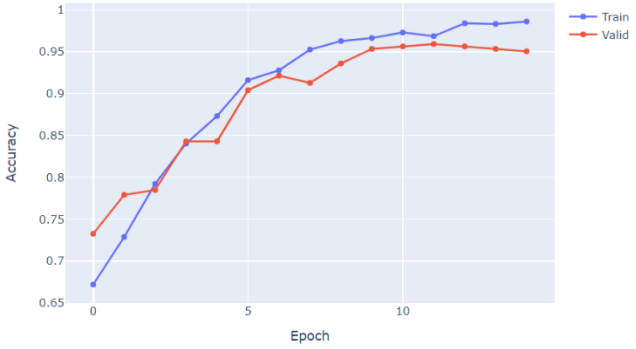

Figure 1.c: Accuracy vs. Epoch of appearance of consolidation

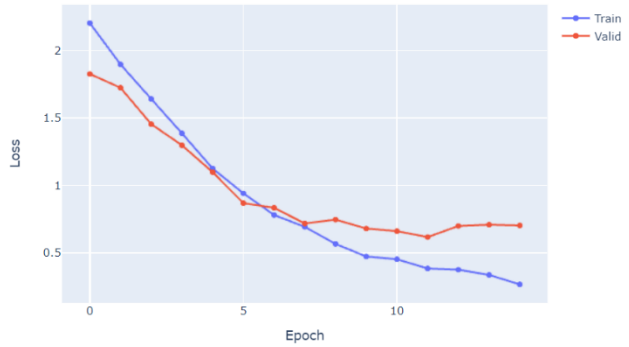

Figure 1.d: Loss vs. Epoch

(37)

Modeling of biological processes using subthreshold electrical circuits

Marah Matar[1], Bayan Khalil[1], Ilan Oren[1], Daniel Ramez[1]

[1]Faculty of Biomedical Engineering, Technion - IIT, Haifa, Israel

Introduction: The modeling of biology stochastics behavior on software-based simulators for example use pseudorandom generators, system clocks, and noise models which significantly increase the simulation time and inhibit scaling for large complex biology processes. The main objective of the project is to address the above challenges by providing a Cytomorphic-based analog circuit for fast and scalable modeling of biology processes with sufficient accuracy. Biological systems in living cells include a repeating basic gene computing unit. The unit was named Perceptgene. The Perceptgene analog circuit can be configured for modeling different biological processes and be used as a building block for a modular emulating system. This project is about the perceptgene circuit designe.

Methods: The proposed analog circuit for implementing the Perceptgene consist of 3 sub circuits:

1. Power circuit – to implement the power (n1, n2) function over X1, X2 inputs.
2. Multiplication circuit – to multiply the output of the power circuits.
3. Activation function – a decision making circuit based of Michaelis-Menten equation.

The perceptgene building blocks circuits were implemented using tower 0.18um process. The circuits were tuned to work with very low currents in order to operate at the subthreshold region and thus function as trans-linear circuits. We used MATLAB and virtuoso environments to analyze the circuits' equations and compare it to the lab measurements of a biological process. In order to build Artificial Neural Networks (ANN), basic classifiers were implemented using the Perceptgene analog circuit and trained with a dedicated algorithm.

Results: spice-virtuoso simulations of the Perceptgene circuit resulted the expected behavior of multiplication, power and activation function include an additional constant marked as K coefficient. The Perceptgene circuit has been used to model a basic genetic process which was previously tested in the lab and the electrical simulation results of the Perceptgene showed a good match to the genetic process lab measurements.

The basic classifiers which were build using the circuit are AND/OR classifiers. These classifiers were implemented using a single neuron ANN realized by Perceptgene circuit, in order to build ANN network.

Conclusions: The Perceptgene analog circuit was designed using trans-linear circuits that operate in the subthreshold region which insures ultra-low power consumption and enable the expansion of the circuit

for large scale biological process simulations. Electrical simulations of the Perceptgene circuit showed a good matching to lab measurements of a basic biology process it was modeling. Since the Perceptgene is configurable, these results proved the potential of the Perceptgene circuit to model other biological processes.

SPICE electrical simulations of the Perceptgene circuit showed that the Perceptgene can implement basic classification functions. These results prove the potential of the Perceptgene circuit as a building block for ANNs, that might enable the implementation of complex biology emulators or other ultra-low power AI systems.

Keywords: Genetic process, Analog Circuit, Modeling concept, Emulation of biology stochastics.

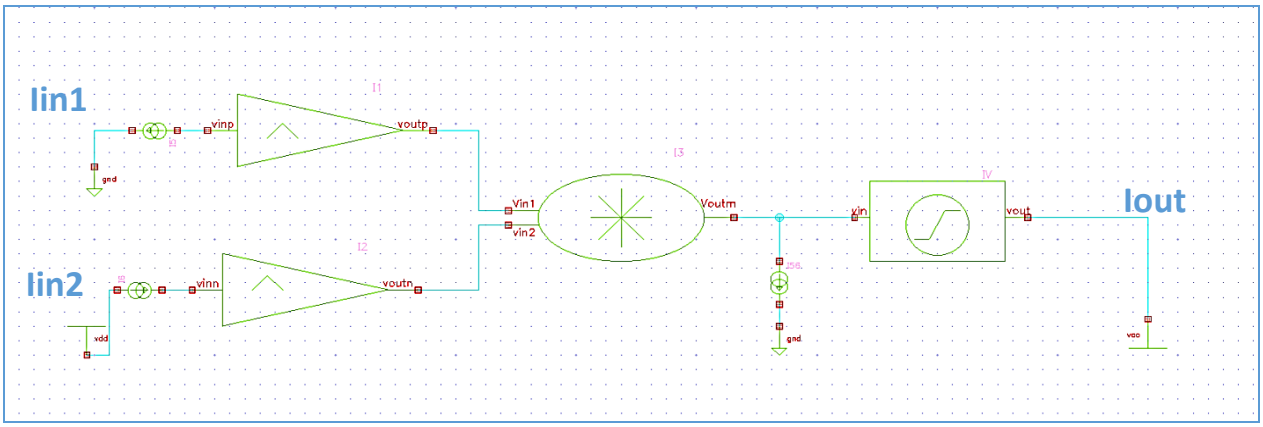

Figure 1: Full Perceptgene circuit

(38)

Determining the Involvement of the Future-Reading Network in Processing Narratives from Age 5 to 18 Years Using Functional Connectivity Approach

Narmeen Haj[2], Tamara Rohana[2], Raya Meri[1], Michal Zivan[1], Tzipi Horowitz-Kraus[1,2]

[1]Educational Neuroimaging Center, Faculty of Education in Science and Technology, Technion – IIT, Haifa, Israel

[2]Faculty of Biomedical Engineering, Technion – IIT, Haifa, Israel

Introduction: Narrative comprehension is a linguistic ability that emerges early in life and has a critical role in language development, in addition to reading acquisition and comprehension. According to the Simple View of Reading model, proficient reading is acquired through intact decoding and linguistic comprehension. Several brain networks are essential for the reading process, including semantic, phonological, visual, syntactic and executive functions networks, which comprise the reading network, and are overlapping with networks involved in processing narratives. The aim of the current study is to determine the involvement of the reading network in processing narratives from pre reading age to proficient reading age using functional connectivity approach.

Methods: In this longitudinal study, thirty-two healthy children ages 5-18 years were annually scanned during a story listening task. The children enrolled at ages 5, 6 or 7 and were scanned for up to 12 years. Behavioral age-appropriate batteries were administered to the children in several time-points during the study. Changes in within and between functional connectivity of the sub-networks that comprise the reading network (i.e., the semantic, phonological, visual, syntactic and executive functions networks) were calculated and compared between the years.

Results: A hierarchical linear regression analysis for all the years, revealed that in year 1 model, the sub-networks related to basic language processing (i.e., visual, phonological, syntactic) accounted for 32.5% of the variation in reading ability prediction as measured in the behavioral reading test in year 6 (ages 12-14 years), and this value amplified to 97.4% in year11 with the involvement of more complex networks (i.e., executive functions). When examining the variation in reading ability prediction as measured in the behavioral reading test of year 11, it was revealed that in year 3 model, the basic sub-networks accounted for 70.4% of the variation for the reading ability. Whereas in more advance years, we revealed a noticeable involvement of more complex networks, such as EF, as in year 9 model they accounted 92.4% of the variation for the reading ability prediction.

Conclusion: Our results come in line with our hypothesis, as we demonstrated that sub-networks of the future-reading network are highly involved in processing narratives. Our findings reveal that along the years, basic sub-networks are involved earlier in processing narratives, and more complex sub-networks (such as executive functions) contribute later to this process, which all together contribute to proficient reading abilities.

Keywords: Reading; Narrative Comprehension; Longitudinal Data, Child Development.

Figure 1: Functional connectivity matrices

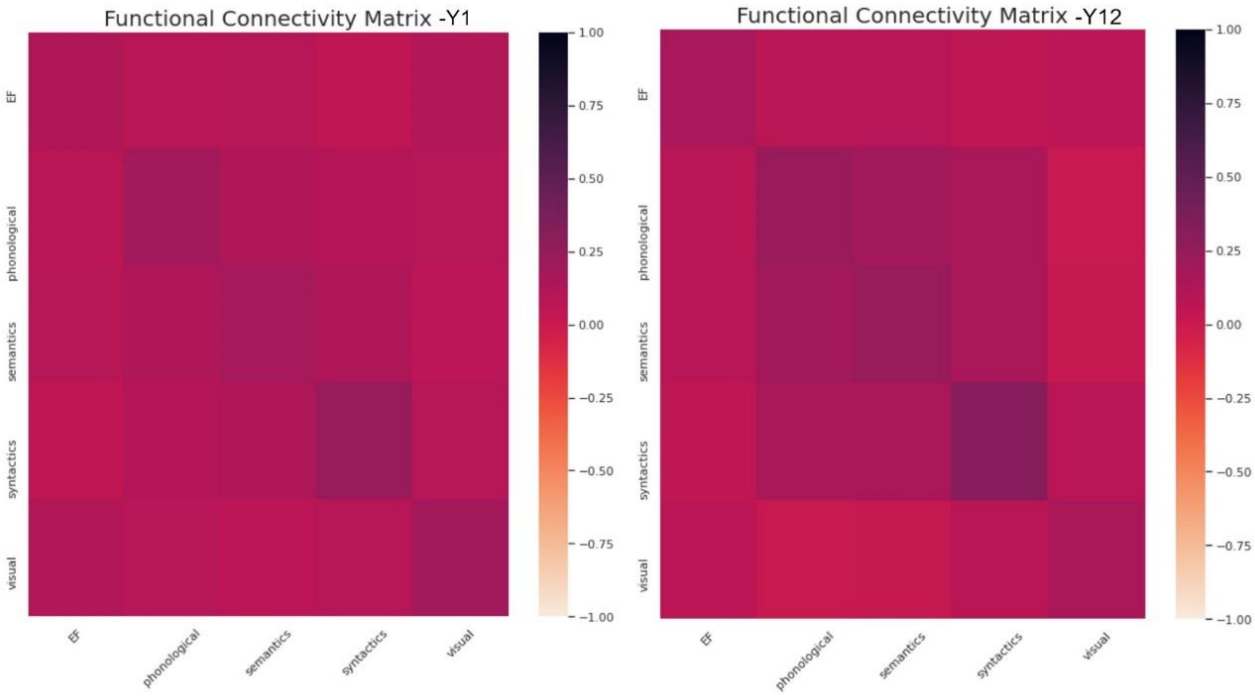

Figure 1: Matrices presenting the within and between networks functional connectivity along the years of the sub-networks that comprise the reading network.
Left to Right images: year 1, year 12.

נכבדיי,

אנו גאים ומתכבדים לקבל את פניכם להשתתפות בכנס: "הצגת הפרויקט השנתי 2021 של הפקולטה להנדסה ביו-רפואית".

מפגש זה מביא לשיאו ניסיון מחקר ופיתוח שנתי של תלמידי השנה הרביעית שלנו. נהוג לומר במסורת העברית: "אין חכם כבעל ניסיון", שפירושו "ניסיון מביא חוכמה". זה בקליפת אגוז, מהות מפעל הפרויקטים. במהלך חווית פיתוח הפרויקט שלהם, הסטודנטים שלנו נאלצו לעבור את כל השלבים הדרושים כדי להגשים רעיון. החל מבעיה רפואית שעימה הם נאלצו להתמודד, הם נאלצו לאמץ את דמיונם ולחשוב "מחוץ לקופסה" על מנת להגיע לפתרון חדש ובר ביצוע. ואז הם נאלצו לשלב את הידע שצברו במהלך הלימודים. ידע זה מקיף את כל ההיבטים של הנדסה ביו-רפואית, כלומר שילוב רקע רפואי עם מיומנויות הנדסיות וידע מדעי. היה צריך ליישם את כל החבילה הזו בכדי לספק פתרון של עולם אמיתי.

אנו מאמינים כי ניסיון מעשי זה חשף והכין את בוגרינו לתעשיית הביו-רפואה ולמגוון רחב של מחקרים ביו-רפואיים בצורה חזקה מאוד המעודדת עבודה רב תחומית החיונית לקריירה העתידית של הסטודנטים, ובנוסף לפיתוח גם של כישורי היזמות שלהם.

בחוברת זו מוצגים תקצירי כל הפרויקטים שהוצגו לעיונכם. אנו בטוחים שהסטודנטים להוטים להציג את תוצאות הפרויקטים שלהם לאורך שנה. אנו מאחלים לכולם קריירה מתגמלת לאחר סיום הלימודים. אנו מקווים שבקרוב מאוד הם ייקחו חלק פעיל בפרויקטים דומים כמדריכים מקצועיים מהתעשייה ומהאקדמיה.

ברכות חמות,

פרופ' חיים אזהרי, דיקן הפקולטה

פרופ"ח נתנאל קורין, האחראי לקורס

כנס פרויקטים

30/6/2021

תקצירים

הפקולטה להנדסה ביו-רפואית
הטכניון - מכון טכנולוגי לישראל